EMILY ANE DIONIZIO DA SILVA

# INFLUENCE OF CLIMATE, FIRE AND PHOSPHORUS IN THE DYNAMICS OF VEGETATION IN THE AMAZON-CERRADO BORDER SIMULATED WITH INLAND MODEL

Dissertação apresentada à Universidade Federal de Viçosa, como parte das exigências do programa de Pós-Graduação em Meteorologia Aplicada, para obtenção do título de Magister Scientiae.

VIÇOSA
MINAS GERAIS-BRASIL
2015

EMILY ANE DIONIZIO DA SILVA

**INFLUENCE OF CLIMATE, FIRE AND PHOSPHORUS IN THE DYNAMICS OF VEGETATION IN THE AMAZON-CERRADO BORDER SIMULATED WITH INLAND MODEL**

Dissertação apresentada à Universidade Federal de Viçosa, como parte das exigências do Programa de Pós-Graduação em Meteorologia Aplicada, para obtenção do título de *Magister Scientiae*.

APROVADA: 12 de fevereiro de 2015.

Fabiana Rita do Couto Santos

Júlio César Lima Neves
(Coorientador)

Marcos Heil Costa
(Orientador)

**Ficha catalográfica preparada pela Biblioteca Central da Universidade Federal de Viçosa - Câmpus Viçosa**

T
S586i
2015

Silva, Emily Ane Dionizio da, 1989-
Influence of climate, fire and phosphorus in the dynamics of vegetation in the Amazon-Cerrado border simulated with INLAND model / Emily Ane Dionizio da Silva. – Viçosa, MG, 2015.
xvii, 75f. : il. (algumas color.) ; 29 cm.

Inclui apêndice.
Orientador: Marcos Heil Costa.
Dissertação (mestrado) - Universidade Federal de Viçosa.
Referências bibliográficas: f.64-72.

1. Ecologia vegetal. 2. Cerrado. 3. Amazonia. 4. Vegetação e clima. 5. Vegetação - Efeito do fogo. 6. Solos - Teor de fósforo. 7. Plantas - Nutrição mineral. I. Universidade Federal de Viçosa. Departamento de Engenharia Agrícola. Programa de Pós-graduação em Meteorologia Aplicada. II. Título.

CDD 22. ed. 581.7

Aos meus pais César Henrique da Silva e
Gercilane Fonseca Dionizio da Silva

## AGRADECIMENTOS

A Deus por me capacitar a cada dia e por me fazer ter a certeza de que tudo está sob Seu controle, por me dar paciência e cuidar de mim.

À minha família, por todo amor e por todo investimento a mim concedido, pelos valores morais e éticos ensinados cuidadosamente ao longo da minha vida. Eu amo demais vocês.

A meu querido Fernando Carvalho por todos os minutos de atenção, por todo amor e esforço realizado para estar junto de mim nesses dois anos. Por cada conselho amigo e palavra de ânimo nas longas ligações noturnas e por todos os abraços quentinhos nas chegadas aos sábados de manhã.

Ao professor Marcos Heil Costa por me receber tão bem e acreditar no meu potencial, por me dar a oportunidade de trabalhar em um grupo de excelência como o Grupo de Pesquisa em Interação Atmosfera-Biosfera. Ao professor Júlio Cesar Lima Neves por me coorientar, e me ensinar pacientemente essa ciência tão nova para mim que é a ciência de solos.

À Universidade Federal de Viçosa e ao Departamento de Engenharia Agrícola por me dar a oportunidade de desenvolver esse trabalho, não só pelo espaço físico, mas por todos os ensinamentos transmitidos.

À Fundação de Amparo à Pesquisa do estado de Minas Gerais (Fapemig), pela concessão da bolsa de estudos.

Aos colaboradores Dra. Andrea Castanho, Dra. Beatriz Marimon, Dr. Ben Hur, Dr. Eddie Lenza, Dra. Mercedes Bustamante, por me concederem dados e informações que possibilitaram a realização desta pesquisa. Agradeço também pelas sugestões e comentários construtivos realizadas por cada um nas visitas ao Mato-Grosso e Fortaleza.

Aos meus amigos do Grupo de Pesquisa em Interação Atmosfera-Biosfera - Ana Beatriz, Carla Camargos, Matheus Lucas, Gabriel Abrahão, Gabrielle Pires (Gabis), Lívia Cristina, Patrícia Porta Nova, Victor Benezoli, Francisca Zenaide, Fabiana Couto (Fabi), Vítor Fontes, Fernando Pimenta, Telmo Sumila, Angélica Patarroyo e Pauline pela disponibilidade em ajudar sempre (principalmente com meus scripts e senhas que sempre somem ou travam), pelos "cafés" e principalmente pela amizade.

Aos meus amigos e colegas do INPE o qual sempre foram atenciosos e solidários ao longo desta caminhada, auxiliando quando necessário nos aspectos pessoais e profissionais.

A nossa secretária Graça, por sua eficiência e carinho.

As minhas amigas de república, Mayana, Naysa, Glenda, Helen, Fernanda, Priscila pela amizade, pelo convívio, pela paciência e por transformarem nossa casa em um "lar", vocês foram essenciais em cada etapa deste trabalho. Aos meus amigos Wellington e Neto por sempre estarem presentes me alegrando com suas companhias.

# BIOGRAFIA

EMILY ANE DIONIZIO DA SILVA, filha de Gercilane Fonseca Dionizio da Silva e Cesar Henrique da Silva, nasceu em 09 de agosto de 1989 na cidade de Guaratinguetá, no estado de São Paulo. Em Fevereiro de 2006 ingressou no curso de Ciências Biológicas nas Faculdades Integradas Teresa D´Ávila (FATEA).

Em 2009 iniciou sua iniciação científica no Instituto Nacional de Pesquisas Espaciais (INPE) no Centro de Ciência do Sistema Terrestre (CCST) na cidade de Cachoeira Paulista, São Paulo, por onde atuou durante os dois anos pós-graduada.

Em abril de 2013 iniciou o curso de Mestrado em Meteorologia Aplicada, no Departamento de Engenharia Agrícola da Universidade Federal de Viçosa (UFV).

## CONTENTS

**LIST OF SYMBOLS** ..... viii

**LIST OF FIGURES** ..... ix

**LIST OF TABLES** ..... xi

**LIST OF ACRONYSMS** ..... xii

**ABSTRACT** ..... xiv

**RESUMO** ..... xvi

**GENERAL INTRODUCTION** ..... 1

**CHAPTER 1 – Phosphorus in the soil and plants – development of a phosphorus regional dataset** ..... 5

**1.1 INTRODUCTION** ..... 5

**1.2 MATERIALS AND METHODS** ..... 8

1.2.1 Data Description of phosphorus in soil ..... 8

1.2.2 Description of the phosphorus regional data ..... 8

1.2.3 Estimating $P_{total}$ from $P_{-Mehlich-1}$ ..... 12

1.2.4 Development and description of the phosphorus regional dataset (PR) ..... 15

1.2.5 Description of the global phosphorus dataset (PG) ..... 16

1.2.6 Development of $V_{max}$ regional and global datasets ..... 17

**1.3 RESULTS** ..... 19

1.3.1 Estimates of total phosphorus ..... 19

1.3.2 Main differences between phosphorus datasets used in this study ..... 21

1.3.3 $V_{max}$ maps used in this study ..... 22

**1.4 CONCLUSIONS** ..... 24

**CHAPTER 2 – Effects of climate, fire and phosphorus in the Amazon-Cerrado border simulated with INLAND model – Numeric experiment development** ..... 25

**2.1 INTRODUCTION** ..... 25

**2.2 MATERIALS AND METHODS** ..... 28

2.2.1 Description of the INLAND Surface Model ..... 28

2.2.2 Model Configuration and Experiment Design ..... 31

2.2.3 Analysis of the Model Sensitivity ..... 33

2.2.4 Determination of the best model configuration ..... 35

2.2.5 Development of the MODIS LAI Map ..... 35

2.2.6 Statistical Analyses ..... 36

**2.3 RESULTS AND DISCUSSION** ..... 37

2.3.1 Comparison of simulations (Isolated Effects) ..... 37
2.3.1.1 Climate effects ..... 37
2.3.1.2 Phosphorus effect ..... 42
2.3.1.3 Fire Effect ..... 45
2.3.3 Longitudinal gradient of biomass and leaf area index in the Amazonia-Cerrado transition – Comparison between simulations and field observations ..... 50
2.3.4 Simulated composition of vegetation ..... 54
**2.4 CONCLUSIONS** ..... 60
**3. GENERAL CONCLUSIONS** ..... 62
**4. REFERENCES** ..... 64
**5. APPENDIX A** ..... 73

# LIST OF SYMBOLS

| | |
|---|---|
| C | Carbon |
| cm | Centimeter |
| m | Meters |
| $m^2$ $m^{-2}$ | Square meter per square meter |
| mm $yr^{-1}$ | Millimeter per year |
| mg | Milligram |
| mg $L^{-1}$ | Milligram per liter |
| mg $dm^{-3}$ | Milligram per cubic decimeter |
| mg $kg^{-1}$ | Milligram per kilogram |
| µmol | Micromolar |
| $m^2$ | Square meter |
| s | Seconds |
| P | Phosphorus |
| N | Nitrogen |
| kg | Kilogram |
| kg $m^{-2}$ | Kilogram per square meter |
| yr | Year |

# LIST OF FIGURES

**Figure 1.** Location and geographical distribution on the regional dataset $P_{total}$ (Quesada et al., 2010) showing the areas of phosphorus sample collection of $P_{-Mehlich-1}$ in Mato Grosso state. The pink dots are locations of sampling and the thick black line is the geographical limit of the Cerrado biome. .....10

**Figure 2.** $P_{total}$ regional dataset in mg $kg^{-1}$ (Quesada et al., 2010) (a), PR with new estimated $P_{total}$ data (b), In both datasets the limit of the Cerrado biome is defined by the thick black line. The sites that provided additional phosphorus data are represented by pink dots. .....16

**Figure 3.** Map of total phosphorus (mg $kg^{-1}$) in the soil (Yang et al., 2013). .....17

**Figure 4.** Difference between the global $P_{total}$ maps and regional $P_{total}$ map (PG-PR) in mg $kg^{-1}$. The Cerrado biome is delimited by the thick black line. .....22

**Figure 5.** Default $V_{max}$ value of INLAND – PC (a), Regional $V_{max}$ dataset – PR (b), Global $V_{max}$ dataset – PG (c), all in $\mu molCO_2\ m^{-2}\ s^{-1}$. .....23

**Figure 6.** INLAND model structure. .....30

**Figure 7.** Map of the average dry season (July, August and September) leaf area index of MODIS product MOD15A2 from 2000 to 2008 and the five transects used in this study. .....36

**Figure 8.** Climate variability effect on NPP, biomass, $LAI_{upper}$ and $LAI_{lower}$. The hatched areas indicate that the variables are statistically different compared to the control simulation at the level of 95% according to the t- test and the thick black line is the geographical limit of the Cerrado biome.....39

**Figure 9.** Regional Phosphorus effect (PR) on NPP (a); biomass (b); $LAI_{upper}$ (c); and $LAI_{lower}$ (d). The hatched areas indicate that the variables are significantly different compared to the control simulation at the level of 95% according to the t- test and the thick black line is the geographical limit of the Cerrado biome. .....44

**Figure 10.** Global Phosphorus effect (PG) on NPP (a); biomass (b); $LAI_{upper}$ (c); and $LAI_{lower}$ (d). The hatched areas indicate that the variables are significantly different compared to the control simulation at the level of 95% according to the t- test and the thick black line is the geographical limit of the Cerrado biome. .....45

**Figure 11.** Fire effect on biomass, $LAI_{upper}$, and $LAI_{lower}$ for all soil phosphorus. The hatched areas indicate that the variables are significantly different compared to the control simulation at the level of 95% according to the t- test and the thick black line is the geographical limit of the Cerrado biome.....47

**Figure 12.** Longitudinal gradient of the dry season leaf area index ($LAI_{dry}$ – MODIS) and biomass (Nogueira et al., 2014) for the transects 1 to 4 (a) and transect 5 (b).....49

**Figure 13.** Results of the vegetation composition when incorporated the effects of nutritional limitation, fire and $CO_2$ in CA and simulated pattern of dominant vegetation. .....58

**Figure 14.** Results of the vegetation composition when incorporated the effects of nutritional limitation, fire and $CO_2$ in CV and simulated pattern of dominant vegetation. .....59

# LIST OF TABLES

**Table 1.** Phosphorus content data ($P_{\text{-Mehlich-1}}$) and clay percentage for each sample collected in the Amazon-Cerrado transition region. ..... 10

**Table 2.** Estimates made for obtaining $P_{\text{-Mehlich-1}}$ values for the stations used in this study. ..... 15

**Table 3.** $P_{total}$ estimates for the 54 soil samples $P_{\text{-Mehlich-1}}$ in the Mato-Grosso..... 19

**Table 4.** $V_{max}$ values and $P_{total}$ values for samples in the Amazon-Cerrado transition region..... 23

**Table 5.** Simulations with different combinations of the factors evaluated by INLAND model considering the climate scenario CA, climatological average (1961-1990). ..... 32

**Table 6.** Simulations with different combinations of the factors evaluated by INLAND model considering the climate scenario CV, 1948-2008 monthly data. ..... 32

**Table 7.** Individual and combined effects for each simulation. ..... 34

**Table 8.** NPP estimates from the INLAND and the relative errors for the KM67, ZF-2, UFAC, CAX, TAM, ZAR and AGP sites. ..... 38

**Table 9.** Correlation coefficients of dry season LAI simulated by INLAND and remote sensing estimates by MODIS. ..... 50

**Table 10.** Correlation coefficients of biomass simulated by INLAND and field estimates biomass (Nogueira et al., 2014). ..... 51

# LIST OF ACRONYSMS

| | |
|---|---|
| C | Clay |
| BESM | Brazilian Earth System Model |
| CA | Average climate (climatology 1961-1990) |
| CENTURY | Model of plant-soil nutrient cycling |
| CLM | The Community Land Model |
| CMAP | Maximum capacity of the soil adsorption |
| $CO_2$ | Carbon Dioxide |
| CTEM | Canadian Terrestrial Ecosystem Model |
| CV | Variable climate (database 1948-2008) |
| DGVMs | Dynamic Global Vegetation Models |
| F | Fire |
| GPP | Gross primary productivity |
| HCL | Hydrochloric acid |
| IBIS | Integrated BIosphere Simulator |
| IGBP | International Global Biosphere Programme |
| INLAND | Integrated Model of Surface Process |
| ISAM | Integrated Science Assessment Model |
| JPL | Lund-Potsdam-Jena Dynamic Global Vegetation Model |
| $LAI_{upper}$ | Upper canopy leaf area index |
| $LAI_{lower}$ | Lower canopy leaf area index |
| $LAI_{dry}$ | Dry season leaf area index (MODIS) |
| LSM | Land Surface Model |
| MODIS | Moderate Resolution Imaging Spectroradiometer |
| NPP | Net primary production |
| $P_{\text{-Mehlich-1}}$ | Phosphorus extracted by Mehlich-1 extractor |
| $P_{\_m1\_est}$ | Estimated Phosphorus extracted by Mehlich-1 extractor |
| $P_{Adc}$ | Phosphorus added in each soil sample |
| PC | Control Phosphorus |
| PFT | Plant functional type |
| PG | Global Phosphorus |
| PR | Regional phosphorus |
| $P_{rem}$ | Remanescent phosphorus |

| | |
|---|---|
| $P_{resin}$ | Phosphorus extracted by Resin |
| $P_{total}$ | Phosphorus total in the soil |
| Rubisco | Ribulose-bisfosfato carboxilase oxigenase |
| UNEMAT | State University of Mato Grosso |
| $V_{max}$ | Maximum rate of carboxylation Rubisco |
| PROBIO | Brazil - National Biodiversity (PROBIO) Project |

## ABSTRACT

SILVA, Emily Ane Dionizio da, M. Sc. Universidade Federal de Viçosa, February, 2015. **Influence of climate, fire and phosphorus in the dynamics of vegetation in the Amazon-Cerrado border simulated with INLAND model.** Adviser: Marcos Heil Costa. Co-Adviser: Júlio Cesar Lima Neves.

Studies to assess the main factors responsible for the dynamics of vegetation in the Amazon such as climate and / or deforestation suggest the possibility of the Amazon rainforest may not resist a potencial change in rainfall patterns, and be converted to an ecosystem of more sparse vegetation like savanna, which gave rise to the term "Amazon Savannization". Some of these initial studies, however, used only future climate scenarios, neglecting in their majority the fire effects and especially the effect of nutrient limitation on vegetation dynamics. Recently, in the context of climate modeling, advancements have been made in an attempt to build models that incorporate the nutritional restriction effect and the fire to assess and measure their effects on vegetation at a large scale. In this work, the main objective was to evaluate the isolated and combined effects of climate (inter annual variability and $CO_2$), fire (F) and nutritional limitation by phosphorus (P) using the dynamic vegetation model INLAND in the transition between forest-Cerrado. The INLAND model is the first Brazilian model to simulate the vegetation dynamics incorporating these factors. The INLAND characterizes the vegetation through plant functional types, which combined differently give rise to biomes. The nutritional limitation is established through a linear function of the total phosphorus content in the soil and the maximum carboxylation capacity of Rubisco enzyme ($V_{max}$). The Rubisco is the main enzyme responsible for regulating carboxylation rates in plants with the C3 photosynthetic mechanism type acting directly on net primary productivity (NPP) and the increase of biomass. Two regional the datasets of $V_{max}$ to be used as input data of the simulations, based on regional (PR) (field measurements) and global data (PG) of total P content in the soil. In the design of numerical experiment, 24 simulations were performed for different combinations of climate factors, P, F and $CO_2$ were obtained. To validate the simulations, regional datasets of dry season leaf area index (LAI), and biomass were compared against simulated values by the INLAND model. The results showed that isolation, the effect of fire on the NPP in the Cerrado is positive and higher than the effects of nutritional restriction, contrary to what happens in the Amazon biome where the P acts to reduce the NPP. The $CO_2$ when evaluated in combination with the effects of fire acted as an

attenuator increasing the NPP in the transition region. With respect to the climate, the use of inter-annual variability improved representation of biomass and LAI simulated by INLAND. The LAI and biomass simulated values showed good correlation with Amazon-Cerrado observed gradient. The best representation of the vegetation composition by INLAND was found when the effects of PG+F+$CO_2$ were combined.

## RESUMO

SILVA, Emily Ane Dionizio da, M. Sc. Universidade Federal de Viçosa, Fevereiro de 2015. **Influência do clima, fogo e fósforo na dinâmica da vegetação na fronteira Amazônia-Cerrado simulada pelo modelo INLAND.** Orientador: Marcos Heil Costa. Coorientador: Júlio Cesar Lima Neves

Estudos realizados para avaliar os principais fatores responsáveis pela dinâmica da vegetação na Amazônia tais como clima e/ou desmatamento sugerem a possibilidade da floresta Amazônica não resistir a uma eventual mudança do regime de chuvas, e ser transformada em um ecossistema de vegetação mais esparsa, do tipo savana, o que deu origem ao termo "Savanização da Amazônia". Parte destes estudos iniciais no entanto utilizavam apenas cenários de climas futuros, negligenciando na maior parte das vezes o efeito do fogo, e principalmente o efeito da limitação nutricional na dinâmica da vegetação. Recentemente, no âmbito da modelagem climática, grandes avanços têm sido realizados na tentativa de se construir modelos que incorporem o efeito da limitação nutricional e do fogo de forma que se possa avaliar e dimensionar os efeitos dos mesmos na vegetação em larga escala. Neste trabalho, o principal objetivo foi avaliar os efeitos isolados e combinados do clima (variabilidade interanual e $CO_2$), fogo (F) e limitação nutricional por fósforo (P) utilizando o modelo de vegetação dinâmica INLAND na transição entre Amazônia-Cerrado. O modelo INLAND é o primeiro modelo brasileiro que permite simular a dinâmica da vegetação incorporando estes fatores. O INLAND caracteriza a vegetação através de tipos funcionais de planta, que combinados de forma diferente dão origem aos biomas. A limitação nutricional no modelo é estabelecida através de uma função linear entre o teor de fósforo total no solo e a capacidade máxima de carboxilação da enzima Rubisco ($V_{max}$). A Rubisco é a principal enzima responsável por regular as taxas de carboxilação nas plantas com mecanismo fotossintético do tipo C3 atuando diretamente na produtividade primária líquida (NPP) e no incremento de biomassa. Dois mapas de Vmáx foram elaborados para serem utilizados como dados de entrada nas simulações, baseados em dados regionais (PR) (medidas de campo) e globais (PG) de teor de P total no solo. No delineamento do experimento numérico, 24 simulações foram realizadas de forma que diferentes combinações entre os fatores clima, P, F e $CO_2$ fossem obtidas. Para validação das simulações, um mapa de índice de área foliar (LAI) MODIS e dados de

biomassa foram contrastados com valores simulados pelo modelo INLAND. Os resultados demonstraram que isoladamente, o efeito do fogo sobre a NPP no Cerrado é positivo e maior em relação aos efeitos da limitação nutricional, contrariamente ao que acontece na região Amazônica onde o P atua na diminuição da NPP. O $CO_2$ por sua vez quando avaliado combinadamente aos efeitos do fogo demonstrou-se como um amenizador, aumentando a NPP na região de transição. Com relação ao clima, o uso de uma variabilidade inter-anual melhorou a representação dos valores de NPP, biomassa e LAI pelo INLAND. Os valores de LAI e biomassa simulados apresentaram boa correlação com os dados observados de forma que o gradiente de vegetação Amazônia - Cerrado conseguiu ser representado. A melhor representação da composição da vegetação pelo modelo INLAND foi quando considerado os efeitos de PG+F+$CO_2$.

## GENERAL INTRODUCTION

On a global scale, the distribution of different forms of existing vegetation is in general controlled by the climate where the relations between precipitation and temperature determine the structural patterns of vegetation (Whittaker, 1975). At a regional level however, these structural patterns of vegetation can still depend on local environmental conditions imposed by local variations in soils, and topography.

The boundaries between the Amazon forest and the Brazilian Cerrado, for example, are not only characterized by a seasonal rainfall gradient, but also influenced in large part by the occurrence of fire, availability of water and nutrients in the soil, herbivory and soil characteristics (Lehmann et al., 2011; Murphy and Bowman, 2012; Sankaran et al., 2004). Due to the impossibility of manipulating some of these factors in their natural environments, it is difficult to assess and quantify the degree of interaction between these various factors and to infer how each of them works on the regional vegetation. Therefore, Dynamic Global Vegetation Models (DGVMs) have been used to isolate and manipulate factors like climate, fire and nutrients, to understand the large-scale effects of these factors on vegetation (Favier et al., 2004; Hirota et al., 2010; House et al., 2003).

The first modeling studies to assess the function of the dynamics of vegetation in the Amazon were developed solely on the basis of climate, deforestation, and $CO_2$ fertilization (Betts et al., 2004; Cox et al., 2000; Oyama and Nobre, 2003; Shukla et al., 1990). These modeling studies indicated that the Amazon rainforest might experience eventual changes in rainfall patterns and either transforms in an ecosystem with more sparse, vegetation savanna like, which gave rise to the term "savannization of the Amazon" (Betts et al., 2004; Cox et al., 2000; Oyama and Nobre, 2003; Salazar et al.,

2007) or tends towards a seasonal forest (Malhi et al., 2009). These pioneering studies were of paramount importance to the advancement of terrestrial biosphere modeling, but in general, the models commonly used by the scientific community have more realistic representations of temperate and cold climate ecosystems, rather than tropical ecosystems. In tropical regions, the DGVMs neglected important factors such as the effects of fire and nutritional limitations.

In the tropics, fire performs an important ecological role on the Earth's surface and influences the productivity of ecosystems, biogeochemical cycles, and the distribution of biomes by changing the biological activity of plants, including their phenology and physiology (Wright, 2005). Recently, Couto-Santos et al. (2014) demonstrated the effects of the fire occurrence on climate dominance in the dynamics of forest-savanna boundaries, in the northern region of the Brazilian Amazon. These authors showed that, in wet years, the forest advanced over the savannas, while in years with lower rainfall, the forest receded and the savanna expanded due the trend of increased frequency of climatic events, such as drought and fire. In the boundary regions between forest and savanna, fire and climate directly influence the growth rates of the vegetation and, depending on the frequency and intensity, may result in increased mortality of trees in a forest and transformation of an undisturbed forest in an inflammable one (Hoffmann et al., 2012). However, to evaluate the dynamic forest-savanna more broadly, in addition to considering the effects of fire, one also must recognize the importance of nutritional limitations on the growth (productivity) of trees.

Studies support that in tropical forests like the Brazilian Amazon, phosphorus (P) is the main limiting nutrient in the productivity of trees instead of nitrogen (Aragão et al., 2009; Davidson et al., 2004; Goll et al., 2012; McGrath et al., 2001; Mercado et

al., 2009; Paoli et al., 2008; Reich et al., 1995; Silver et al., 1994; Wang et al., 2010). Phosphorus is a nutrient that has not been incorporated in most of DGVMs such as the LPJ (Lund-Potsdam-Jena Dynamic Global Vegetation Model) (Sitch et al., 2003; Smith et al., 2001), the CLM (The Community Land Model) (Oleson et al., 2004), or the ISAM (The Science Integrated Model Assessment) (Jain and Yang, 2005; Jain et al., 1996, 2006). In general, only the nitrogen cycle has been used by DGVMs to limit the productivity in ecosystems. The lack of information on the spatial distribution of phosphorus in the soil in its different forms was a major factor that made the implementation of P nutrient in global climate models difficult (Yang and Post, 2011; Yang et al., 2013). However, recent works such as Quesada et al. (2009, 2010, 2011), Yang and Post (2011) and Yang et al. (2013) provided a comprehensive database of physical and chemical properties of the soil in the Amazon region, and global maps of P content in the soil in its different forms. Then, it is currently possible to implement the P content in the soil and to include the nutrient limitation in the productivity in the DGVM IBIS (Integrated Biosphere Simulator) model (Castanho et al., 2013; Yang et al., 2014).

The IBIS model was used as base for the development of the INLAND (Integrated Model of Land Surface Processes). The INLAND model is a Brazilian DGVM able to represent characteristics and important process in South America biomes. The nutritional restriction (Castanho et al., 2013) and fire (Arora and Boer, 2005) on vegetation were recently implemented in this model, which makes it a potential tool for investigating the dynamics of vegetation in Brazilian ecosystems.

Using the INLAND model, this study aimed to evaluate the isolated and combined effects of phosphorus, climate and fire on productivity, leaf area index (LAI),

and biomass increment of vegetation in the Amazon-Cerrado transition, and checking the performance of the model in simulating the Amazon-Cerrado current position. These work is organized in two chapters: Chapter 1: Estimates of total phosphorus in the soil for use in INLAND; Chapter 2: Description and analysis of simulations to evaluate the current position of the Amazon-Cerrado border considering the different phosphorus effects, fire in the current climate scenarios and comparing with leaf area index (LAI MODIS) and biomass values for longitudinal transects in the Amazon-Cerrado boundaries.

# CHAPTER 1 – Phosphorus in the soil and plants – development of a phosphorus regional dataset

## 1.1 INTRODUCTION

In tropical forests like in the Brazilian Amazon, phosphorus (P) is the main limiting nutrient in the productivity of trees instead of nitrogen (Aragão et al., 2009; Davidson et al., 2004; Goll et al., 2012; McGrath et al., 2001; Paoli et al., 2008; Reich et al., 1995; Silver et al., 1994; Wang et al., 2010). In plants, P has an essential role as part of energy-rich compounds such as adenosine triphosphate (ATP) used by most physiological processes such as photosynthesis (Malavolta, 1985). In contrast to nitrogen, which is derived primarily from the atmosphere, phosphorus arises out of rocks and generally presents a high content in younger soils, becoming scarcer in older soils due to weathering processes that lead to the formation of aluminum and iron oxides which are strong adsorbers of P in the soil (Uehara and Gilman, 1981).

This high adsorption capacity is the reason why the tropical soils are strictly poor in available P forms, maintenance P by plants occurring mainly via an intra-cycling system, where the plant absorbs most of the nutrients from the decomposition of its own litter, stems, trunks and the death of fine roots (Waring and Schlesinger, 1985). Besides the intra-cycling system, a physiological mechanism known as biogeochemical cycling, assists in maintaining the phosphorus content in most plants by carrying P from older, photosynthetically inactive tissues to young growing tissues with high capacity (Poggiani, 1981) as a way to minimize losses to soil P through the adsorption process. According to Switzer and Nelson (1973) about 40% of the N, P and K can be recycled through this mechanism. Recently works such as Mercado et al. (2011) and Quesada et al. (2012) relate the P content in the leaves with the maximum carboxylation capacity of

Rubisco enzyme ($V_{max}$) and the P content in the soil with the woody structure of tropical forests, reinforcing the close relationship between tropical vegetation and the different fractions of P (foliar and soil). In the soil, phosphorus is present in diverse forms that vary according to the chemical nature of the compounds to which it is connected, as well as its binding energy. The different forms of phosphorus found in soil include: labile inorganic phosphorus and organic phosphorus (which are the forms available to plants), occluded phosphorus, phosphorus mineral secondary, phosphorus in the form of apatite and the total phosphorus ($P_{total}$) (Yang et al., 2013). According to Quesada et al. (2012), total soil P was a better predictor of wood production rates in Amazonia than any of the fractionated organic phosphorus or inorganic phosphorus pools, suggesting that it is not only the immediately available P forms, but probably the entire soil phosphorus pool that is interacting with forest growth on longer timescales.

Based on this finding Castanho et al. (2013) obtained a linear relationship between the $P_{total}$ content in the soil and the $V_{max}$ values for woody plants in the Amazon, so that the amount of net primary productivity was spatially limited by $P_{total}$ content in the soil throughout the Amazon Basin. The nutritional limitation of P in woody plants was restricted to Amazonia due to the lack of $P_{total}$ content measurements for Cerrado.

This chapter has three objectives: (1) to develop a model for estimating the amount of $P_{total}$ from measurements of soil available P content in the Cerrado region on the Amazon-Cerrado transition area located in the state of Mato Grosso, thus expanding the $P_{total}$ regional dataset prepared by Castanho et al. (2013); (2) to develop a new dataset of $V_{max}$ from the $P_{total}$ regional dataset and (3) to generate a second dataset of $V_{max}$ based on a global P database (Yang et al., 2013). These $V_{max}$ datasets will be used

in the next chapter for photosynthesis limitation in the experiment with the INLAND model.

## 1.2 MATERIALS AND METHODS

The methodology described in this chapter includes: (1) Description of the phosphorus regional data; (2) Estimation of $P_{total}$ from phosphorus $P_{-Melich-1}$; (3) Development of dataset of $P_{total}$ (PR); (4) Development of two $V_{max}$ datasets from regional (PR) and global (PG) databases, for use by INLAND;

### 1.2.1 Data Description of phosphorus in soil

In Soil Science, numerous extractors that use different methodologies to extract the lability of the forms of P in the soil are commonly used. In this study, we used P data obtained via the Mehlich-1 extractor ($H_2SO_4$, 0.025mol $L^{-1}$ + HCl 0.05mol $L^{-1}$) 1:10 soil: solution ratio ($P_{-Melich-1}$), and the resin method ($P_{resin}$) databases to estimate total phosphorus ($P_{total}$).

The Mehlich-1 extractor has been performing reasonably well as an indicator of the availability of P in the soil and with the application of soluble phosphate fertilizers. The method of resin anion-exchange is an attempt to reproduce in the laboratory the P absorption process by the plants in the field. The Hedley fractionation (Hedley and Stewart, 1982) uses sequentially extracts from lower to higher desorption power and allow the separation of P forms according to their nature (organic or inorganic) and facility of desorption (Cross and Schlesinger, 1995). This method consists of a sequential extraction of reagents of increased strength.

### 1.2.2 Description of the phosphorus regional data

We used 54 samples of phosphorus content (P) in the soil, where 52 were obtained via the Mehlich-1 extractor, and two were direct measurements of total phosphorus content ($P_{total}$) in the soil. In addition to these samples collected in the field, a soil map of the Amazon was also used (Quesada et al., 2010).

The 54 samples of P content were provided by researchers group at the UNEMAT – State University of Mato Grosso, collected for different vegetation types ranging from sparse physiognomies like Campo de Murundus, open flooded field, Cerrado típico to more dense forest formations such as Cerradão, semideciduous forest, evergreen seasonal forest and gallery forest in the Amazon-Cerrado transition region in the state of Mato Grosso (Table 1).

The information on Cerradão, Cerrado típico, Cerrado rupestre and Gallery Forest are from the Bacaba Municipal Park conservation area, which is located in Nova Xavantina-MT (14° 41'S and 52° 20'W). The Bacaba Municipal Park has 489 ha of natural landscape with Cerrado vegetation type with the prevalence of Cerrado sensu-stricto, with medium to clayey soil texture (Marimon Junior and Haridasan, 2005). For the physiognomies open field and Campo de Murundus, the phosphorus samples are from the Araguaia State Park, located in the northeast of Mato Grosso State, in the municipality of Novo Santo Antonio (11° 37' 02"S and 50° 40' 10"W), inserted in the extensive sedimentary plain of Bananal in the Araguaia River basin.

The spatial distribution of these samples can be seen in Figure 1, which represents the total phosphorus in the soil with a spatial resolution of 1° × 1° (Quesada et al., 2010).

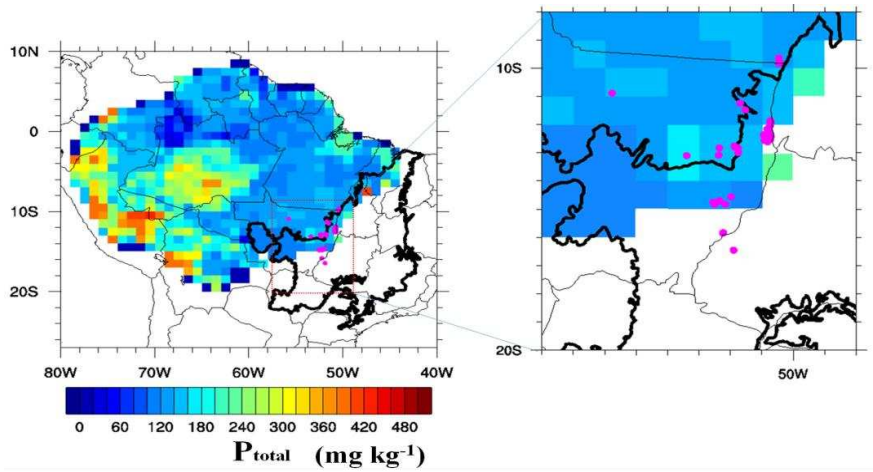


**Figure 1.** Location and geographical distribution on the regional dataset $P_{total}$ (Quesada et al., 2010) showing the areas of phosphorus sample collection of $P_{\text{-Mehlich-1}}$ in Mato Grosso state. The pink dots are locations of sampling and the thick black line is the geographical limit of the Cerrado biome.

**Table 1.** Phosphorus content data ($P_{\text{-Mehlich-1}}$) and clay percentage for each sample collected in the Amazon-Cerrado transition region.

| Location | | | Physiognomy | Phosphorus | Clay |
|---|---|---|---|---|---|
| Latitude | Longitude | n | | mg kg$^{-1}$ | % |
| -15.55 | -50.10 | 1 | Cerrado rupestre[a] | 0.89 | 30.6 |
| -15.54 | -50.10 | 2 | Cerrado típico[b] | 0.20 | 34.7 |
| -14.17 | -51.76 | 3 | Cerrado ralo[c] | 2.28 | 21.1 |
| -14.17 | -51.77 | 4 | Cerrado ralo[c] | 1.30 | 30.0 |
| -14.15 | -51.76 | 5 | Cerrado típico[b] | 2.93 | 40.5 |
| -14.16 | -51.77 | 6 | Cerrado típico[b] | 1.11 | 35.4 |
| -14.71 | -52.35 | 7 | Cerrado típico[b] | 3.00 | 35.8 |
| -14.71 | -52.35 | 8 | Cerrado típico[b] | 0.84 | 48.2 |
| -14.71 | -52.35 | 9 | Cerrado típico[b] | 0.42 | 49.3 |
| -14.82 | -52.17 | 10 | Semi deciduous Forest | 3.18 | 21.5 |
| -14.71 | -52.35 | 11 | Cerrado típico[b] | 0.34 | 17.3 |
| -14.71 | -52.35 | 12 | Cerrado típico[b] | 0.13 | 17.7 |
| -14.70 | -52.35 | 13 | Cerradão[d] | 0.26 | 21.0 |
| -14.70 | -52.35 | 14 | Cerradão[d] | 0.10 | 24.4 |
| -14.69 | -52.35 | 15 | Cerradão[d] | 5.46 | 21.0 |
| -14.69 | -52.35 | 16 | Cerradão[d] | 3.80 | 33.5 |
| -14.69 | -52.35 | 17 | Cerradão[d] | 1.90 | 40.5 |
| -14.69 | -52.35 | 18 | Cerradão[d] | 0.80 | 44.0 |

**Table 1.** (Continued.)

| Location | | | Physiognomy | Phosphorus | Clay |
|---|---|---|---|---|---|
| **Latitude** | **Longitude** | **n** | | **mg kg$^{-1}$** | **%** |
| -14.69 | -52.35 | 19 | Cerradão[d] | 0.30 | 45.2 |
| -14.72 | -52.36 | 20 | Gallery Forest | 0.87 | 15.0 |
| -14.72 | -52.36 | 21 | Gallery Forest | 6.94 | 10.5 |
| -14.72 | -52.36 | 22 | Flooded Gallery Forest | 1.71 | 11.7 |
| -13.10 | -53.39 | 23 | Flooded Riparian Forest | 26.0 | 43.0 |
| -13.10 | -53.39 | 24 | Flooded Riparian Forest | 18.0 | 49.0 |
| -13.00 | -50.25 | 25 | Cerrado rupestre[a] | 2.44 | 4.44 |
| -12.38 | -50.93 | 26 | Campo de Murundus[g] | 2.30 | 39.3 |
| -12.36 | -50.93 | 27 | Campo de Murundus [g] | 3.30 | 29.5 |
| -12.56 | -50.92 | 28 | Campo de Murundus [g] | 3.30 | 22.0 |
| -12.04 | -50.73 | 29 | Campo de Murundus [g] | 0.70 | 38.5 |
| -12.57 | -50.91 | 30 | Campo de Murundus [g] | 1.70 | 39.1 |
| -12.62 | -50.82 | 31 | Campo de Murundus [g] | 2.40 | 25.6 |
| -12.43 | -50.72 | 32 | Campo de Murundus [g] | 2.30 | 29.1 |
| -12.22 | -50.77 | 33 | Campo de Murundus [g] | 2.30 | 30.8 |
| -12.37 | -50.94 | 34 | Campo de Murundus [g] | 5.20 | 37.5 |
| -12.37 | -50.94 | 35 | Campo de Murundus [g] | 4.00 | 39.3 |
| -12.38 | -50.93 | 36 | open flooded field | 1.60 | 32.5 |
| -12.38 | -50.93 | 37 | open flooded field | 2.00 | 20.8 |
| -12.36 | -50.93 | 38 | open flooded field | 1.60 | 17.1 |
| -12.04 | -50.73 | 39 | open flooded field | 0.80 | 22.8 |
| -12.57 | -50.91 | 40 | open flooded field | 0.70 | 25.0 |
| -12.62 | -50.82 | 41 | open flooded field | 2.20 | 20.8 |
| -12.43 | -50.72 | 42 | open flooded field | 1.60 | 19.6 |
| -12.22 | -50.77 | 43 | open flooded field | 1.90 | 27.0 |
| -12.37 | -50.94 | 44 | open flooded field | 3.10 | 29.9 |
| -12.37 | -50.94 | 45 | open flooded field | 0.90 | 30.8 |
| -12.83 | -52.35 | 46 | Seasonal Evergreen Forest | **$P_{total}$= 141** | 49.0 |
| -12.81 | -51.85 | 47 | Seasonal Evergreen Forest | **$P_{total}$= 117** | 16.0 |
| -11.18 | -50.23 | 48 | Cerrado denso[h] | 2.71 | 3.96 |
| -11.18 | -50.23 | 49 | Cerradão[d] | 1.66 | 4.16 |
| -11.17 | -50.23 | 50 | Cerrado típico[b] | 1.45 | 3.56 |
| -11.86 | -50.72 | 51 | open flooded field | 2.00 | 41.6 |

**Table 1.** (Continued.)

| Location | | | Physiognomy | Phosphorus | Clay |
|---|---|---|---|---|---|
| Latitude | Longitude | n | | mg $kg^{-1}$ | % |
| -11.86 | -50.72 | 52 | Campo de Murundus [g] | 2.80 | 47.7 |
| -9.11 | -54.23 | 53 | Cerrado rupestre[a] | 4.17 | 4.56 |
| -9.79 | -50.43 | 54 | Semi deciduous Forest | 2.04 | 18.4 |

[a]**Cerrado rupestre**: a tree-shrub vegetation that grows in areas of accentuated topography with many rock outcrops and shallow soils, where individual trees establish themselves in clefts in the rocks so that their densities will vary as a function of the specific conditions of each site (Ribeiro and Walter, 2008).

[b]**Cerrado típico**: a vegetation of trees and shrubs fairly regular and usually not exceeding 4 meters (Ribeiro and Walter, 2008).

[c]**Cerrado ralo**: a vegetation that is more open than Cerrado típico; the trees not exceeding 2 to 3 meters in height, covering from 5 to 20% of the soil (Ribeiro and Walter, 2008).

[d]**Cerradão**: a dense and tall woodland formation (Ribeiro and Walter, 2008).

[g]**Campo de Murundus**: a typical landscape of Central Brazil characterized by countless rounded earth mounds (the 'murundus'), which are covered by woody 'Cerrado' vegetation and are found scattered over a grass-covered surface (the 'campo') (Ribeiro and Walter, 2008).

[h]**Cerrado denso:** this vegetation is more dense than Cerrado típico; the trees exceeding 2 to 3 meters in height, and covered with a woody cover ranging from 10 to 60% (Ribeiro and Walter, 2008).

### 1.2.3 Estimating $P_{total}$ from $P_{\text{-Mehlich-1}}$

The data for the phosphorus content in soil extracted by Mehlich-1 ($P_{\text{-Mehlich-1}}$) was used to estimate the total phosphorus content in the soil ($P_{total}$). For this, it was first necessary to establish a relationship between $P_{\text{-Mehlich-1}}$ and $P_{total}$.

Based on $P_{\text{-Mehlich-1}}$ studies conducted by Neves (2000) and dos-Santos et al. (2008), a linear relationship was produced between $P_{\text{-Mehlich-1}}$, clay percent and $P_{total}$ using a Hedley fractionation database for 26 sites in the Amazon (Castanho et al., 2013; Quesada et al., 2010). These 26 locations were the same used to construct the relationship between $V_{max}$ and $P_{total}$ by Castanho et al. (2013). The database of Quesada et al. (2010) provides data of physicochemical properties of the soil, and Hedley fractionation data with eight different fractions of phosphorus content in the soil, including: phosphorus extracted by resin ($P_{resin}$), inorganic bicarbonate, organic bicarbonate, inorganic sodium hydroxide, organic sodium hydroxide, hydrochloric acid,

$P_{total}$ and residual. The location, name of the experimental sites, value of $P_{total}$, $P_{Resin}$ and clay percent used to establish the relationship between $P_{\text{-Mehlich-1}}$ and $P_{total}$ are shown in Table A1 (Appendix Table A1).

Based on the Freire (2001) equation, the amount of phosphorus remaining in the soil, i.e., the existing amount of P in the soil ($P_{rem}$) was estimated for each site, based on their clay content:

$$P_{rem} = 52.44 - 0.9646\ C + 0.005\ C^2 \qquad R^2 = 0.747 \qquad (1)$$

where $P_{rem}$ is expressed in mg $L^{-1}$ and C is the clay content in %. $P_{rem}$ is the P concentration that remains in solution after shaking soil with 0.01 mol $L^{-1}$ $CaCl_2$ containing 60 mg $L^{-1}$ P (Alves and Lavorenti, 2006).

After obtaining of the remaining values ($P_{rem}$), it was necessary to estimate the phosphorus maximum adsorption capacity (CMAP) of each soil, in order to calculate how much phosphorus each soil is capable of adsorbing.

Based on significative data from several studies (Bognola, 1995; Campello et al., 1994; Fabres, 1986; Gonçalves, 1988; Ker, 1995; Moreira, 1988; Muniz, 1983; Novelino, 1999; Paula, 1993), Neves (2000) proposed Equation (2) to calculate CMAP from $P_{rem}$:

$$CMAP = 1816.1 - 373.72\ \log P_{rem} \qquad R^2 = 0.751 \qquad (2)$$

where CMAP is expressed in mg $kg^{-1}$ and $P_{rem}$ in mg $L^{-1}$.

Knowing the CMAP, Neves (2000) also proposed a robust model (Equation 3), which estimates how much the Mehlich-1 extractor is capable of removing of P added in each soil sample ($P_{\text{-Mehlich-1}}/P_{Adc}$). This relationship was adjusted based on 31 soil

samples data from the work of Bahia-Filho (1982), Muniz (1983), Gonçalves (1988) and Novelino (1999);

$$\frac{P_{-Mehlich-1}}{P_{Adc}} = 380.96 \ \ CMAP^{-1.2101} \qquad R^2 = 0.734, (p<0.001) \qquad (3)$$

where $P_{Adc}$ is the added dose of P in soil expressed in mg $kg^{-1}$.

Finally, knowing $P_{\text{-Mehlich-1}}/P_{Adc}$, $P_{resin}/P_{\text{-Mehlich-1}}$ was estimated using the Equation (4) established by Neves (2000) with r=0.899, n=26.

$$\frac{P_{resin}}{P_{-Mehlich-1}} = 0.5553 \ \left(\frac{P_{-Mehlich-1}}{P_{Adc}}\right)^{0.6002} \qquad R^2 = 0.808, (p<0.001) \qquad (4)$$

where $P_{resin}$ is expressed in mg $kg^{-1}$.

With the $P_{resin}$ values and the ratio estimated by Equation (4), $P_{\text{-Mehlich-1}}$ values for all stations in Quesada et al. (2010) were estimated ($P_{\_m1\_est,}$ expressed in mg $kg^{-1}$). Table 2 shows the estimates obtained by Equations (1), (2), (3) and (4) for the 26 sites in the Amazon.

Obtaining $P_{\_m1\_est}$ values for locations where data for clay content and $P_{total}$ (mg $kg^{-1}$) were available, enabled the development of a linear regression model (Equation 5) that estimates $P_{total}$ from $P_{\_m1\_est}$ (mg $kg^{-1}$) and C (%) with r = 0.639.

$$P_{total} = 72.4628 + 0.639 \ \left(P_{\_m1\_est} \ C\right) \qquad R^2 = 0.408, (p<0.001) \qquad (5)$$

Although the $R^2$ value is low, the regression is significant at p<0.01. The product ($P_{\_m1\_est}$ C) was used to correct the effect of soil clay contribution on $P_{\text{-Mehlich-1}}$ values, which tends to remove smaller amounts of P, for high values of clay. Applying the Equation (5) to the data presented in Table 1, $P_{total}$ was estimated for all field samples collected in Mato Grosso. These results are presented in Table 3 in Section 1.3 (Results

and Discussion) and were incorporated to the regional dataset of Quesada et al. (2010), described in section 1.2.4.

**Table 2.** Estimates made for obtaining $P_{\text{-Mehlich-1}}$ values for the stations used in this study.

| **Observation data** | | | **Estimated data** | | | | |
|---|---|---|---|---|---|---|---|
| Quesada et al. (2010) | | | $\mathbf{P_{resin}}$ | **CMAP** | $\frac{\mathbf{P_{-Mehlich-1}}}{\mathbf{P_{Adc}}}$ | $\frac{\mathbf{P_{resin}}}{\boldsymbol{P_{-\mathbf{Mehlich-1}}}}$ | $\mathbf{P_{\_m1\_est}}$ |
| **Plot** | $\mathbf{P_{resin}}$ | **Clay** | | | | | |
| ID | mg $kg^{-1}$ | % | mg $L^{-1}$ | mg $kg^{-1}$ | mg $kg^{-1}$ | mg $kg^{-1}$ | mg $kg^{-1}$ |
| 'RIO-12' | 3.42 | 9.50 | 43.7 | 404.2 | 0.27 | 1.23 | 2.79 |
| 'ELD-12' | 5.34 | 20.1 | 35.1 | 486.9 | 0.21 | 1.40 | 3.80 |
| 'SCR-01' | 2.36 | 6.88 | 46.0 | 384.9 | 0.28 | 1.18 | 1.99 |
| 'TIP-05' | 9.01 | 37.3 | 23.4 | 637.6 | 0.15 | 1.71 | 5.27 |
| 'JRI-01' | 1.30 | 80.7 | 7.15 | 1081 | 0.08 | 2.51 | 0.52 |
| 'JAS-02' | 8.79 | 29.1 | 28.6 | 563.1 | 0.18 | 1.56 | 5.64 |
| 'CAX-01' | 5.17 | 41.8 | 20.9 | 680.6 | 0.14 | 1.79 | 2.88 |
| 'MBO-01' | 3.14 | 11.5 | 42.0 | 419.1 | 0.26 | 1.26 | 2.49 |
| 'BNT-04' | 4.82 | 57.7 | 13.4 | 845.2 | 0.11 | 2.10 | 2.30 |
| 'TAP-04' | 4.50 | 89.3 | 6.18 | 1136 | 0.08 | 2.60 | 1.73 |
| 'ALP-12' | 7.37 | 14.0 | 40.0 | 437.9 | 0.24 | 1.30 | 5.67 |
| 'SUC-02' | 4.06 | 37.2 | 23.5 | 636.7 | 0.15 | 1.71 | 2.38 |
| 'AGP-01' | 2.99 | 42.6 | 20.4 | 688.8 | 0.14 | 1.81 | 1.66 |
| 'ZAR-03' | 4.81 | 31.1 | 27.3 | 580.7 | 0.17 | 1.60 | 3.01 |
| 'TAP-123' | 1.65 | 66.1 | 10.5 | 936.4 | 0.10 | 2.26 | 0.73 |
| 'ZAR-04' | 7.48 | 18.3 | 36.5 | 471.8 | 0.22 | 1.37 | 5.45 |
| 'JUR-01' | 10.6 | 36.6 | 23.8 | 631.2 | 0.16 | 1.70 | 6.22 |
| 'RST-01' | 8.29 | 25.4 | 31.2 | 530.8 | 0.19 | 1.49 | 5.55 |
| 'ALF-01' | 3.51 | 11.4 | 42.1 | 418.7 | 0.26 | 1.26 | 2.79 |
| 'DOI-01' | 7.18 | 19.1 | 35.9 | 478.5 | 0.22 | 1.39 | 5.18 |
| 'SIN-01' | 2.58 | 9.8 | 43.5 | 406.4 | 0.27 | 1.23 | 2.10 |
| 'TAM-01' | 5.85 | 37.8 | 23.2 | 641.9 | 0.15 | 1.72 | 3.41 |
| 'CUZ-03' | 11.5 | 42.5 | 20.5 | 687.4 | 0.14 | 1.80 | 6.35 |
| 'CRP-01' | 21.8 | 18.1 | 36.7 | 470.1 | 0.22 | 1.37 | 15.9 |
| 'HCC-21' | 7.34 | 25.6 | 31.0 | 532.4 | 0.19 | 1.50 | 4.90 |

### 1.2.4 Development and description of the phosphorus regional dataset (PR)

The 54 $P_{total}$ values were used to extend (Table 3) the map of Quesada et al. (2010) in the Amazon-Cerrado transition. Depending on the spatial distribution of the

samples, the average for the $P_{total}$ values (Table 4) was calculated inside each 1° × 1° pixel and the new values added are shown in Figure 2b.

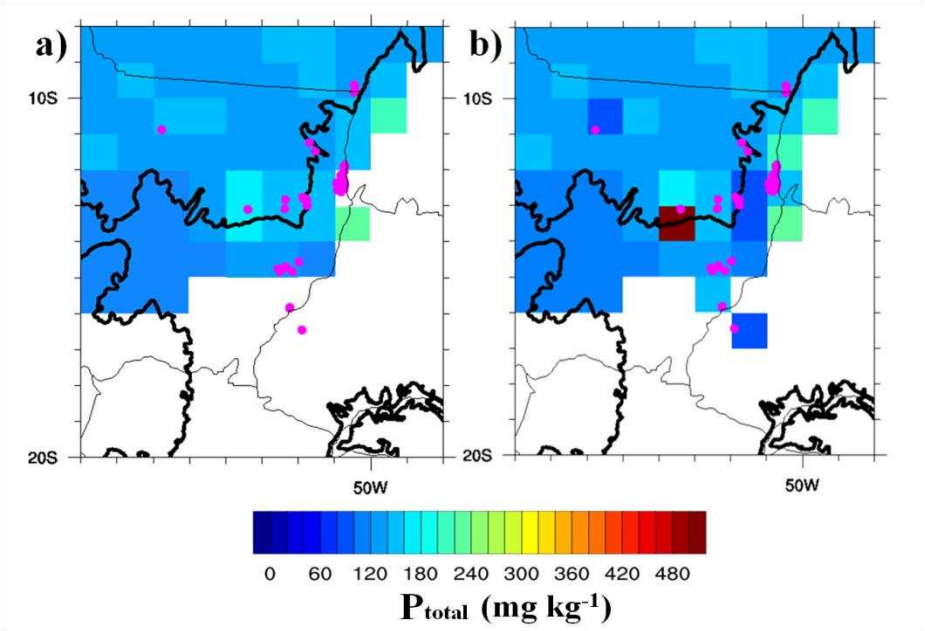


**Figure 2.** $P_{total}$ regional dataset in mg $kg^{-1}$ (Quesada et al., 2010) (a), PR with new estimated $P_{total}$ data (b), In both datasets the limit of the Cerrado biome is defined by the thick black line. The sites that provided additional phosphorus data are represented by pink dots.

### 1.2.5 Description of the global phosphorus dataset (PG)

A global dataset of total phosphorus content in the soil ($P_{total}$) with a spatial resolution of 0.5° × 0.5° was also used (Figure 3), which is part of a database containing six global maps of the different forms of phosphorus found in soil that include: labile inorganic phosphorus, organic phosphorus, occluded phosphorus, secondary mineral phosphorus, phosphorus in the form of apatite and total phosphorus ($P_{total}$) (Yang et al., 2013). These maps were made from lithologic maps, distribution of soil development stages, fraction of the remaining source material for different stages of weathering using chronosequence studies (29 studies), and phosphorus distribution in different forms for

each soil type based on analysis of Hedley fractionation (Yang and Post, 2011) which are part of a worldwide collection of soil profile data.

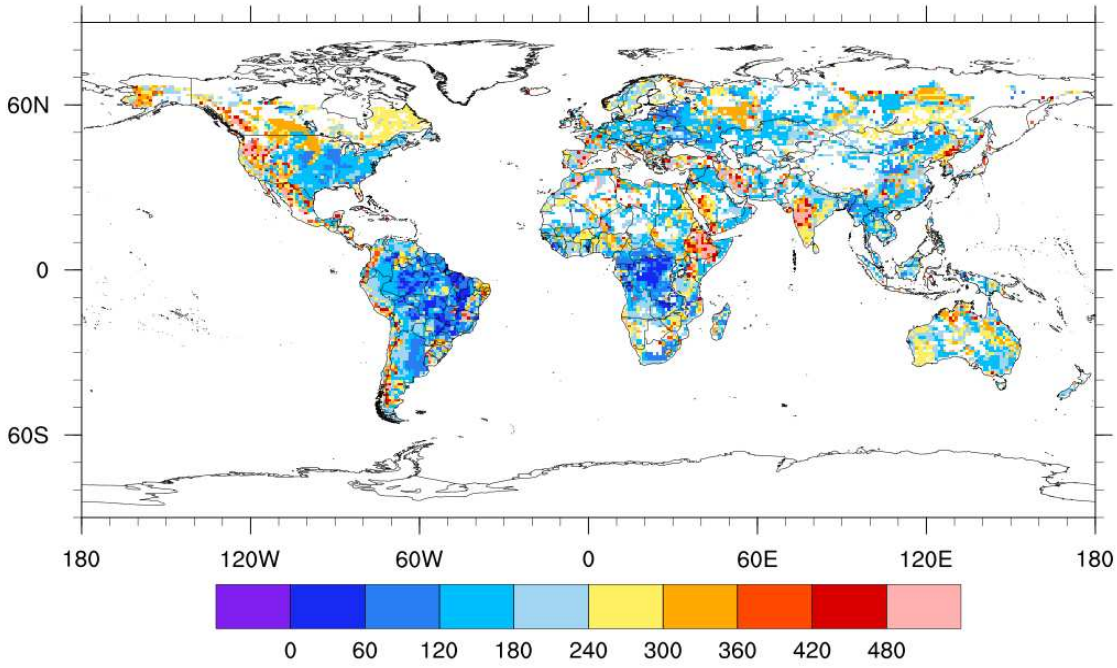


**Figure 3.** Map of total phosphorus (mg $kg^{-1}$) in the soil (Yang et al., 2013).

The uncertainties and limitations of this database are related to the Hedley fractionation data used. When quantified, these uncertainties are 17% for low weathered soils, 65% for intermediate soils and 68% for highly weathered soils (Yang et al., 2013).

### 1.2.6 Development of $V_{max}$ regional and global datasets

The $V_{max}$ values in the INLAND model are defined for each plant functional type which, combined in different forms, create the distinct ecosystems represented by the model. Default $V_{max}$ values for tropical evergreen trees are defined at 65 $\mu molCO_2\ m^{-2}\ s^{-1}$.

Here, the $V_{max}$ datasets were produced through a linear relationship proposed by Castanho et al. (2013), who used soil fertility ($P_{total}$) to limit photosynthesis in the

INLAND model by estimating the maximum capacity of carboxylation by the Rubisco enzyme ($V_{max}$), applying Equation (6) to the regional and global datasets of total phosphorus (PR and PG).

$$V_{max} = 0.1013\ P_{total} + 30.037 \quad (6)$$

where $V_{max}$ and $P_{total}$ are given in $\mu molCO_2\ m^{-2}\ s^{-1}$ and $mg\ kg^{-1}$, respectively.

## 1.3 RESULTS

### 1.3.1 Estimates of total phosphorus

Table 3 shows the total P values estimated for 54 samples of $P_{\text{-Mehlich-1}}$ in Mato Grosso state. These samples were spatialized to a grid of 1° × 1° resolution and resulted in 12 new pixels. Due to the large size of the grid (approximately 111 km), different physiognomies were grouped into a single pixel. For each pixel, the average of $P_{total}$ values was considered regardless of the type of vegetation.

The average values per physiognomy were higher for the Riparian Forest with $P_{total}$ = 11.46 mg $kg^{-1}$ (n=2) followed by Campo de Murundus with $P_{total}$ = 132.8 mg $kg^{-1}$ (n=11), Semi deciduous Forest with $P_{total}$ = 106.3 mg $kg^{-1}$ (n=2), Cerradão with $P_{total}$ = 103.0 mg $kg^{-1}$ (n=8), open flooded field with $P_{total}$ = 100.8 mg $kg^{-1}$ (n=11), Cerrado ralo with $P_{total}$ = 100.2 mg $kg^{-1}$ (n=2), Gallery Forest with $P_{total}$ = 99.8 mg $kg^{-1}$ (n=2), Cerrado típico with $P_{total}$ = 97.1 mg $kg^{-1}$ (n=8), Flooded Gallery Forest with $P_{total}$ = 85.2 mg $kg^{-1}$ (n=1), Cerrado rupestre with $P_{total}$ = 84.62 mg $kg^{-1}$ (n=3), and Cerrado denso with $P_{total}$ = 79.32 mg $kg^{-1}$ (n=1).

**Table 3.** $P_{total}$ estimates for the 54 soil samples $P_{\text{-Mehlich-1}}$ in the Mato-Grosso.

| Location | | | | Phosphorus | $P_{total}$ |
|---|---|---|---|---|---|
| **Latitude** | **Longitude** | **n** | **Physiognomy** | **mg $kg^{-1}$** | **mg $kg^{-1}$** |
| -15.55 | -50.1 | 1 | Cerrado rupestre[a] | 0.89 | 89.9 |
| -15.54 | -50.1 | 2 | Cerrado típico[b] | 0.20 | 76.9 |
| -14.17 | -51.76 | 3 | Cerrado ralo[c] | 2.28 | 103 |
| -14.17 | -51.77 | 4 | Cerrado ralo[c] | 1.30 | 97.4 |
| -14.15 | -51.76 | 5 | Cerrado típico[b] | 2.93 | 148 |
| -14.16 | -51.77 | 6 | Cerrado típico[b] | 1.11 | 97.6 |
| -14.71 | -52.35 | 7 | Cerrado típico[b] | 3.00 | 141 |
| -14.71 | -52.35 | 8 | Cerrado típico[b] | 0.84 | 98.3 |

**Table 3.** (Continued.)

| Location | | | | Phosphorus | $P_{total}$ |
|---|---|---|---|---|---|
| **Latitude** | **Longitude** | **n** | **Physiognomy** | **mg kg$^{-1}$** | **mg kg$^{-1}$** |
| -14.71 | -52.35 | 9 | Cerrado típico[b] | 0.42 | 85.7 |
| -14.82 | -52.17 | 10 | Semi deciduous Forest | 3.18 | 116 |
| -14.71 | -52.35 | 11 | Cerrado típico[b] | 0.34 | 76.2 |
| -14.71 | -52.35 | 12 | Cerrado típico[b] | 0.13 | 73.9 |
| -14.7 | -52.35 | 13 | Cerradão[d] | 0.26 | 76.0 |
| -14.7 | -52.35 | 14 | Cerradão[d] | 0.10 | 74.0 |
| -14.69 | -52.35 | 15 | Cerradão[d] | 5.46 | 146 |
| -14.69 | -52.35 | 16 | Cerradão[d] | 3.80 | 154 |
| -14.69 | -52.35 | 17 | Cerradão[d] | 1.90 | 122 |
| -14.69 | -52.35 | 18 | Cerradão[d] | 0.80 | 95.0 |
| -14.69 | -52.35 | 19 | Cerradão[d] | 0.30 | 81.1 |
| -14.72 | -52.36 | 20 | Gallery Forest | 0.87 | 80.1 |
| -14.72 | -52.36 | 21 | Gallery Forest | 6.94 | 119 |
| -14.72 | -52.36 | 22 | Flooded Gallery Forest | 1.71 | 85.2 |
| -13.1 | -53.39 | 23 | Flooded Riparian Forest | 26.0 | 787 |
| -13.1 | -53.39 | 24 | Flooded Riparian Forest | 18.0 | 636 |
| -13 | -50.25 | 25 | Cerrado rupestre[a] | 2.44 | 79.4 |
| -12.38 | -50.93 | 26 | Campo de Murundus[g] | 2.30 | 130 |
| -12.36 | -50.93 | 27 | Campo de Murundus [g] | 3.30 | 135 |
| -12.56 | -50.92 | 28 | Campo de Murundus [g] | 3.30 | 119 |
| -12.04 | -50.73 | 29 | Campo de Murundus [g] | 0.70 | 89.7 |
| -12.57 | -50.91 | 30 | Campo de Murundus [g] | 1.70 | 115 |
| -12.62 | -50.82 | 31 | Campo de Murundus [g] | 2.40 | 112 |
| -12.43 | -50.72 | 32 | Campo de Murundus [g] | 2.30 | 115 |
| -12.22 | -50.77 | 33 | Campo de Murundus [g] | 2.30 | 118 |
| -12.37 | -50.94 | 34 | Campo de Murundus [g] | 5.20 | 197 |
| -12.37 | -50.94 | 35 | Campo de Murundus [g] | 4.00 | 173 |
| -12.38 | -50.93 | 36 | open flooded field | 1.60 | 106 |
| -12.38 | -50.93 | 37 | open flooded field | 2.00 | 99.0 |
| -12.36 | -50.93 | 38 | open flooded field | 1.60 | 89.9 |
| -12.04 | -50.73 | 39 | open flooded field | 0.80 | 84.1 |
| -12.57 | -50.91 | 40 | open flooded field | 0.70 | 83.6 |
| -12.62 | -50.82 | 41 | open flooded field | 2.20 | 102 |

**Table 3.** (Continued.)

| Location | | | | Phosphorus | $P_{total}$ |
|---|---|---|---|---|---|
| **Latitude** | **Longitude** | **n** | **Physiognomy** | **mg kg$^{-1}$** | **mg kg$^{-1}$** |
| -12.43 | -50.72 | 42 | open flooded field | 1.60 | 92.5 |
| -12.22 | -50.77 | 43 | open flooded field | 1.90 | 105 |
| -12.37 | -50.94 | 44 | open flooded field | 3.10 | 132 |
| -12.37 | -50.94 | 45 | open flooded field | 0.90 | 90.2 |
| -12.83 | -52.35 | 46 | Seasonal Evergreen Forest | | 142 |
| -12.81 | -51.85 | 47 | Seasonal Evergreen Forest | | 117 |
| -11.18 | -50.23 | 48 | Cerrado denso[h] | 2.71 | 79.3 |
| -11.18 | -50.23 | 49 | Cerradão[d] | 1.66 | 76.9 |
| -11.17 | -50.23 | 50 | Cerrado típico[b] | 1.45 | 75.8 |
| -11.86 | -50.72 | 52 | Campo de Murundus [g] | 2.80 | 158 |
| -11,86 | -50,72 | 51 | open flooded field | 2.00 | 126 |
| -9.11 | -54.23 | 53 | Cerrado rupestre[a] | 4.17 | 84.6 |
| -9,79 | -50,43 | 54 | Semi deciduous Forest | 2.04 | 96.4 |

[a]**Cerrado rupestre**: a tree-shrub vegetation that grows in areas of accentuated topography with many rock outcrops and shallow soils, where individual trees establish themselves in clefts in the rocks so that their densities will vary as a function of the specific conditions of each site (Ribeiro and Walter, 2008).

[b]**Cerrado típico**: a vegetation of trees and shrubs fairly regular and usually not exceeding 4 meters (Ribeiro and Walter, 2008).

[c]**Cerrado ralo**: a vegetation is more open than Cerrado típico; the trees not exceeding 2 to 3 meters in height, covering from 5 to 20% of the soil (Ribeiro and Walter, 2008).

[d]**Cerradão**: a dense and tall woodland formation (Ribeiro and Walter, 2008).

[g]**Campo de Murundus**: are a typical landscape of Central Brazil characterized by countless rounded earth mounds (the 'murundus'), which are covered by woody 'Cerrado' vegetation and are found scattered over a grass-covered surface (the 'campo') (Ribeiro and Walter, 2008).

[h]**Cerrado denso:** this vegetation is more dense than Cerrado típico; the trees exceeding 2 to 3 meters in height, and covered with a woody cover ranging from 10 to 60% (Ribeiro and Walter, 2008).

### 1.3.2 Main differences between phosphorus datasets used in this study

Figure 4 shows the difference of the soil phosphorus content between the global $P_{total}$ map (PG) and the regional map (PR). It is possible to observe that the global data underestimates the $P_{total}$ values in some Amazon-Cerrado transitional areas, mainly in western Amazonia. PG overestimations are observed in northern of Amazonia and in most of the Cerrado biome area.

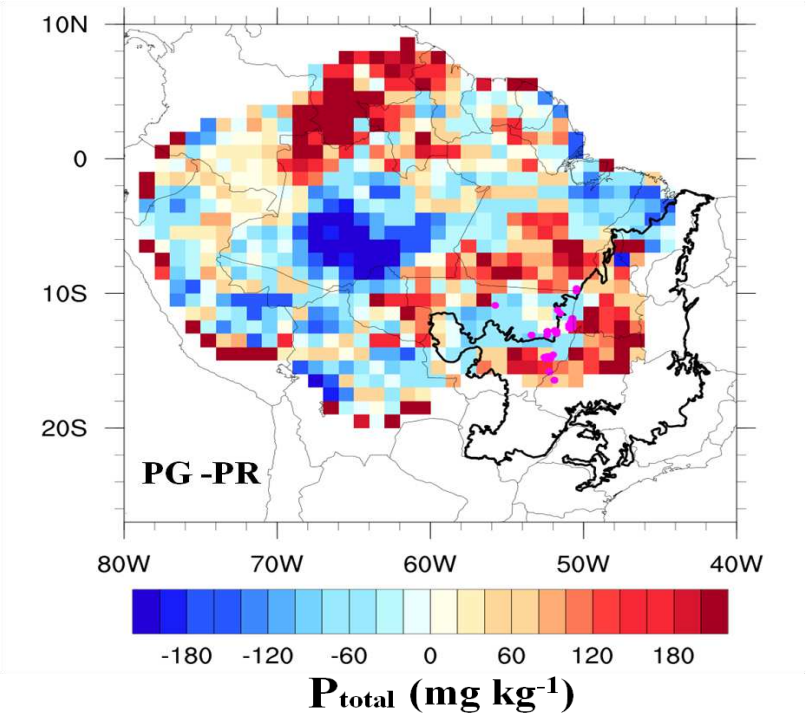


**Figure 4.** Difference between the global $P_{total}$ maps and regional $P_{total}$ map (PG-PR) in mg $kg^{-1}$. The Cerrado biome is delimited by the thick black line.

The differences between the absolute values of total phosphorus at a spatial resolution of 1° × 1° varied in the range of ±180 mg $kg^{-1}$, with an average of 24.19 mg $kg^{-1}$.

### 1.3.3 $V_{max}$ maps used in this study

Equation 6 was applied to the regional map of $P_{total}$ (Section 1.2.6) to obtain the regional $V_{max}$ map (PR), and to the global $P_{total}$ map (Section 1.2.5) to generate the global $V_{max}$ map (PG). Figure 5 shows $V_{max}$ calculated from the P datasets. In Figure 5a, all pixels received the same value for $V_{max}$ (65 µmol$CO_2$ $m^{-2}$ $s^{-1}$), corresponding to the default settings of INLAND. In Figures 5b and 5c it is possible to observe that the $V_{max}$ data followed the spatial gradient of the total P content in soil, with values varying between 36 and 76 µmol$CO_2$ $m^{-2}$ $s^{-1}$.

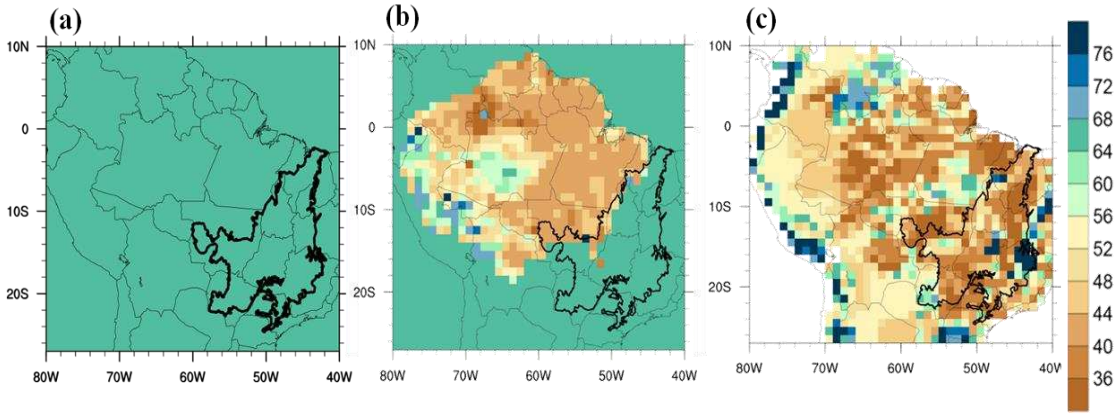


**Figure 5.** Default $V_{max}$ value of INLAND – PC (a), Regional $V_{max}$ dataset – PR (b), Global $V_{max}$ dataset – PG (c), all in $\mu molCO_2\ m^{-2}\ s^{-1}$.

The estimated values of $P_{total}$ in the Amazon-Cerrado border were used to expand the regional P map used by Castanho et al. (2013) and thus generate the $V_{max}$ map shown in Figure 5b. These new values are described in Table 4 and range from 37.9 to 102.1 $\mu molCO_2\ m^{-2}\ s^{-1}$.

**Table 4.** $V_{max}$ values and $P_{total}$ values for samples in the Amazon-Cerrado transition region.

| **Samples** | | **Average $P_{total}$** | **$V_{max}$** |
|---|---|---|---|
| n=54 | Pixel | mg $kg^{-1}$ | $\mu molCO_2\ m^{-2}\ s^{-1}$ |
| 2 | 1 | 83.38 | 38.48 |
| 4 | 2 | 111.6 | 41.34 |
| 16 | 3 | 101.5 | 40.32 |
| 2 | 4 | 711.5 | 102.1 |
| 1 | 5 | 79.39 | 38.08 |
| 20 | 6 | 114.3 | 41.62 |
| 1 | 7 | 141.5 | 44.38 |
| 1 | 8 | 117.0 | 41.89 |
| 3 | 9 | 77.32 | 37.87 |
| 2 | 10 | 141.7 | 44.39 |
| 1 | 11 | 84.61 | 38.61 |
| 1 | 12 | 96.40 | 39.80 |

## 1.4 CONCLUSIONS

The recent availability of phosphorus data in the Amazon made possible the development of a model able to estimate $P_{total}$ throught $P_{\text{-Mehlich-1}}$, thus extending the regional soil map in the Amazon-Cerrado transition. This methodology allows new estimates of $P_{total}$ to be obtained from $P_{\text{-Mehlich-1}}$ data collected in the field, using a robust model with 99% confidence in the estimates.

Although a model was developed to estimate $P_{total}$ in the soil, it is recommended that future works interested in evaluating the P content in the plants should not collect only the labile P, but use the Hedley fractionation method, which informs all forms of P for the given soil sample.

The results produced by the estimates of $P_{total}$ were incorporated into the total phosphorus regional dataset, generating a new map of regional $V_{max}$. The $V_{max}$ maps produced in this work are potentially useful tools to DGVMs in general, and are used in the numeric experiment in the next chapter.

# CHAPTER 2 – Effects of climate, fire and phosphorus in the Amazon-Cerrado border simulated with INLAND model – Numeric experiment development

## 2.1 INTRODUCTION

The transition between the Amazon and Cerrado in Brazil has the largest area of contact between forest and savanna in the tropical regions and these biomes differ fundamentally in their structural characteristics and species composition (Torello-Raventos et al., 2013). In this transition, climate seasonality – especially precipitation – and fire disturbances have an important role in the balance of the vegetation due to influences of the ecological and biogeochemical processes of vegetation directly affecting the carbon fluxes (for example, the Gross Primary Production – GPP, Net Primary Production – NPP and respiration) that, over time, may lead to changes in composition and structure of vegetation (Alves et al., 1997). Tree species associated with forest or savanna vegetation differ in numerous physiological characteristics, such as fire survivorship (Hoffmann et al., 2009; Ratnam et al., 2011), as well as in their wood and foliar characteristics (Gotsch et al., 2010), sometimes related with soil fertility (Ferreira-Ribeiro and Tabarelli, 2002; Miranda et al., 2003; Quesada et al., 2012). Generally, we have an incomplete knowledge on how the trees of these vegetation types differ in photosynthesis characteristics, especially in terms of response to nutrient availability.

In the transition Amazonia-Cerrado there are no studies assessing the influence of factors such as nutritional limitation by P in the photosynthesis rates of woody trees. However, studies that quantify the P levels in soils along the Amazon rainforest in its various forms contribute to information about the P content in the soil (Quesada et al., 2009; Quesada et al., 2010; Quesada et al., 2012; Yang et al., 2013). In Cerrado regions,

the quantification of phosphorus is poor, since it was believed that, in contrast to tropical forests, photosynthetic capacity in the savannas would be more likely to be limited by N than by P (Lloyd et al., 2009).

However, works from West Africa showed that, depending on the relative concentrations of P and N in the leaves, both Rubisco activity and electron transport activity of African savanna and forest trees can potentially be limited by either N or P (Domingues et al., 2010), so there is no consensus about how the vegetation is limited by these nutrients and how this limitation associated with factors such as climate and fire could act on the areas of transition in a scenario of future climate change. Numerous efforts through dynamic vegetation models (DGVMs) have been conducted on Amazonia forests with the aim of understanding dynamics through the analysis of long-term field observations of tree growth and mortality patterns as they relate to climatic and edaphic variations across the basin (Castanho et al., 2013; Phillips et al., 2004; Quesada et al., 2012).

The INLAND model is a DGVM that has been improved by the Brazilian scientific community to better represent intrinsic characteristics of tropical biomes like fire and nutritional limitation. The objective of this chapter is to simulate the current position of the Amazon-Cerrado border, considering different combinations among nutritional limitation, occurrence of fire, interannual climate variability and mean climate to investigate the influence of these factors on the dynamics of the Amazonia-Cerrado transition. The specific objectives are 1) generate a leaf area index (LAI) map for the Amazonia-Cerrado transition for validation of the simulations, 2) compare LAI values and biomass simulated by the model with the values of leaf area index and biomass from MODIS (MOD15A2 product) in five longitudinal transects in the

Amazon-Cerrado boundaries and 3) determine the model configuration that best represents the Amazon-Cerrado transition.

## 2.2 MATERIALS AND METHODS

### 2.2.1 Description of the INLAND Surface Model

The INLAND model is the main and the first land-surface component of the Brazilian Earth System Model (BESM). INLAND is based on the IBIS model (Foley et al., 1996) which considers changes in the composition and structure of vegetation in response to the environment and incorporates important aspects of biosphere-atmosphere interactions in South America. The model simulates the exchanges of energy, water, carbon and momentum between soil-vegetation-atmosphere. These processes are organized in a hierarchical framework and operate at different time steps, ranging from 60 minutes to 1 year, coupling ecological, biophysical and physiological processes (Kucharik et al., 2000). The vegetation is represented by two layers, upper and lower canopy, and 12 plant functional types (PFTs): tropical evergreen trees, tropical deciduous trees, temperate evergreen trees (broadleaf), temperate evergreen trees (conifers), temperate deciduous trees (broadleaf), boreal coniferous evergreen trees, boreal deciduous trees (broadleaf), boreal deciduous trees (coniferous), perennial shrubs, deciduous shrubs, herbaceous C3 and grasses C4. The combination of the 12 PFTs creates the distinct ecosystems represented by the model: tropical evergreen forest, tropical deciduous forest, temperate evergreen broadleaf forest, temperate evergreen conifer forest, temperate deciduous forest, boreal evergreen forest, boreal deciduous forest, mixed forest, savanna, grassland, dense shrubland, open shrubland, tundra, desert and polar desert or ice.

The leaf photosynthesis and respiration are calculated used Farquhar equations (Farquhar et al., 1980; Sharkey, 1985), where the gross photosynthesis rate per unit leaf area (Ag) is a function of absorbed light, leaf temperature, internal carbon dioxide

concentration, and the Rubisco enzyme capacity for photosynthesis ($V_{max}$). The maintenance respiration is a function only of $V_{max}$. The yearly dynamic vegetation module computes the following for each PFT: gross and net primary productivity (GPP and NPP), changes in biomass pools, simple mortality disturbance processes and resultant Leaf Area Index (LAI), thus allowing vegetation type and cover to change through time. GPP and NPP are calculated at the end of each year as:

$$\text{GPP} = \int Ag_{dti} \tag{7}$$

$$\text{NPP} = (1-\eta) \int (Ag, i - R_{leaf,i} - R_{wood,i} - R_{root,i})\, dt \tag{8}$$

where η (0.33) is the fraction of carbon lost in the construction of net plant material because of growth respiration (Amthor, 1984). The partitioning of the NPP for each plant functional type resolves carbon in three biomass pools: leaves, stems and fine roots. The leaf area index (LAI) of each PFT is obtained by simply dividing leaf carbon by specific leaf area, which in INLAND is considered fixed (one value) for each PFT.

The soil physical properties in INLAND used a multilayer formulation of soil (eight soil layers) to simulate the diurnal and seasonal variations of heat and moisture. Each layer is described in terms of soil temperature, volumetric water content and ice content (Foley et al., 1996; Thompson and Pollard, 1995). Furthermore, all of these processes are influenced by these soil texture and amount of organic matter within the soil profile.

Considering these aspects vegetation dynamics and soil physical properties the model can simulate plant competition for light and water between trees, shrubs and herbaceous through shading and differences in water uptake (Foley et al., 1996).

The soil chemical properties are represented by the carbon cycle (C), nitrogen (N) and phosphorus (P), the latter being recently implemented by Castanho et al. (2013). The carbon cycle is simulated through vegetation, litter and soil organic matter, where the biogeochemical module is similar to the CENTURY model (Parton et al., 1993; Verberne et al., 1990). The amount of C existing in the first meter of soil is divided into different compartments characterized according to their time residence, which can vary in an interval of a few hours for microbial biomass and organic material to several years for lignin. For the nitrogen, the model considers only the soil N transformations and carbon decomposition, not influencing the productivity of vegetation, ie., there is a fixed C:N ratio. Phosphorus is used only to limit the net primary productivity. The total phosphorus available in the soil is used to estimate the maximum capacity of carboxylation by the enzyme Rubisco ($V_{max}$) through a linear relationship, Equation 6.

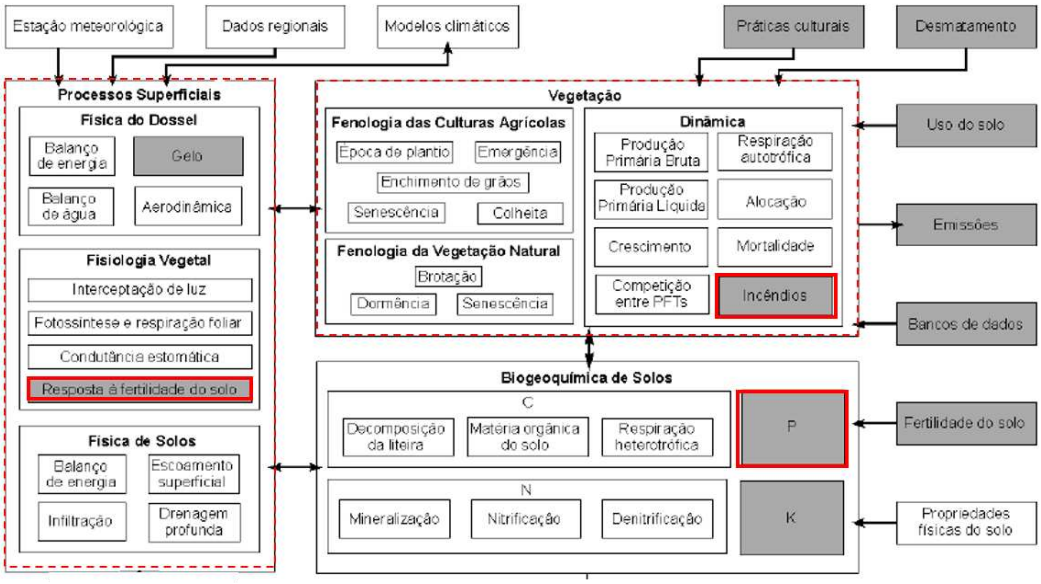


**Figure 6.** INLAND model structure.

INLAND also contains two fire modules. The first module is a simple fixed-value disturbance, which does not depend on the environmental conditions. The second module is based on the fire module of the Canadian model of fire CTEM (Arora and Boer, 2005). In this module, all three aspects of the fire triangle – the availability of fuel to burn, the flammability of vegetation depending on environmental conditions, and the presence of an ignition source – are taken into account. Here, CTEM uses an arbitrary anthropogenic fire probability which is summed to the natural ignition probability.

### 2.2.2 Model Configuration and Experiment Design

The model was forced with a prescribed climate based on the Climate Research Unit (CRU) databases of the University of East Anglia (New et al., 1999). Two boundary conditions were used; the first is referred to as the monthly climatological average (CA), commonly used by the scientific community to represent the average climate of a 30 year period of the last century (1961-1990). The second boundary condition is the historical dataset, used to represent the actual climate variability for the period 1948-2008 (CV), a continuous record of 61 years. The dataset has a 1-degree spatial resolution and a monthly time resolution.

Soil texture data is based on the IGBP-DIS global soil (Global Soil Data Task 2000) (Hansen and Reed, 2000), and the Quesada et al. (2010) dataset. All of the simulations started with the potential vegetation defined by the Center for Sustainability and the Global Environment (SAGE)(Ramankutty and Foley, 1999), with soil carbon and litter pools set to zero.

In the experiment design, the control simulations (PC) to both climate scenarios (CA and CV) considered lack of nutritional limitation per phosphorus, $CO_2$ fixed at

380 ppm and no fire effects (fire module off), for a period of 428 years (equivalent to the period 1581-2008). In the control run (PC) the $V_{max}$ data used to calculate productivity were the default global value used by the dynamic vegetation module of the INLAND (65 $\mu molCO_2\ m^{-2}\ s^{-1}$) for the plant functional types: tropical evergreen trees and tropical deciduous trees. Simulations with different combinations between the climate scenarios (CA and CV), different nutritional limitation scenarios provided by $V_{max}$ maps (PR and PG), fire effects (F) on or off, and the effects of $CO_2$ fixed (380 ppm) or variable $CO_2$ (270 ppm to 385 ppm) were also performed. A summary of the simulations are presented in Tables 5 and 6.

**Table 5.** Simulations with different combinations of the factors evaluated by INLAND model considering the climate scenario CA, climatological average (1961-1990).

| **$CO_2$** | **Fire (F)** | **$V_{max}$** | | |
|---|---|---|---|---|
| | | **PC** | **PR** | **PG** |
| **Fixed** | Off | CA+PC | CA+PR | CA+PG |
| **Fixed** | On | CA+PC+F | CA+PR+F | CA+PG+F |
| **Variable** | Off | CA+PC+$CO_2$ | CA+PR+$CO_2$ | CA+PG+$CO_2$ |
| **Variable** | On | CA+PC+F+$CO_2$ | CA+PR+F+$CO_2$ | CA+PG+F+$CO_2$ |

**Table 6.** Simulations with different combinations of the factors evaluated by INLAND model considering the climate scenario CV, 1948-2008 monthly data.

| **$CO_2$** | **Fire (F)** | **$V_{max}$** | | |
|---|---|---|---|---|
| | | **PC** | **PR** | **PG** |
| **Fixed** | Off | CV+PC | CV+PR | CV+PG |
| **Fixed** | On | CV+PC+F | CV+PR+F | CV+PG+F |
| **Variable** | Off | CV+PC+$CO_2$ | CV+PR+$CO_2$ | CV+PG+$CO_2$ |
| **Variable** | On | CV+PC+F+$CO_2$ | CV+PR+F+$CO_2$ | CV+PG+F+$CO_2$ |

These combinations of the different nutritional limitation scenarios ($V_{max}$), climate (CA or CV, with or without variations of $CO_2$) and fire (F), allow the evaluation of individual and combined effects of climate, soil chemistry, and the incidence of fire

in the NPP, biomass and LAI, and their consequent effect on the position of the Amazon-Cerrado border.

### 2.2.3 Analysis of the Model Sensitivity

Analyses were performed for the individual effects of climate, phosphorus, fire and $CO_2$ on the explanatory variables: Net Primary Production (NPP), biomass, and leaf area index of the upper and lower canopy ($LAI_{upper}$, $LAI_{lower}$).

Analysis of the isolated effect of climate variability was performed using a combination of CV+PC and CA+PC, so that the subtraction between the simulations presents the effect of climate variability isolated: (CV+PC) - (CA+PC) = $(CV\text{-}CA)_{|PC}$; in other words, this is the effect of climate variability for default $V_{max}$ (PC).

The same logic was applied to isolate factors such as fire and phosphorus in different climate scenarios, e.g. the isolated effect of fire with an average climate scenario without influence of nutritional limitation is calculated by the difference between CA+PC+F and CA+PC, so that (CA+PC+F) - (CA+PC) = $F_{|CA\ PC}$. The isolated effect of fire with a climate variability scenario without influence of nutritional limitation is calculated by the difference between CV+PC+F and CV+PC, so that (CV+PC+F) - (CV+PC) = $F_{|CV\ PC}$.

The different combinations of climate scenarios with or without the fire effect and different phosphorus limitations are described in the Table 7. After the analysis of the individual effects, the combined effect was analyzed following the same reasoning, as shown in column E of Table 7.

**Table 7.** Individual and combined effects for each simulation.

| | **Combined Effects** | | | | |
|---|---|---|---|---|---|
| | **A** | **B** | **C** | **D** | **E** |
| | **Climate** | **Phosphorus (P)** | **Fire (F)** | **$CO_2$** | **$CO_2$+F** |
| 1 | (CV+PC)-(CA+PC) | (CA+PR)-(CA+PC) | (CA+PC+F)-(CA+PC) | (CA+$CO_2$+PC)-(CA+PC) | (CA+PC+F+$CO_2$)-(CA+PC) |
| **2** | (CV+PR)-(CA+PR) | (CV+PR)-(CV+PC) | (CV+PC+F)-(CV+PC) | (CV+$CO_2$+PC)-(CV+PC) | (CV+PC+F+$CO_2$)-(CV+PC) |
| **3** | (CV+PG)-(CA+PG) | (CA+PG)-(CA+PC) | (CA+PR+F)-(CA+PR) | (CA+$CO_2$+PR)-(CA+PR) | (CA+PR+F+$CO_2$)-(CA+PR) |
| **4** | | (CV+PG)-(CV+PC) | (CV+PR+F)-(CV+PR) | (CV+$CO_2$+PR)-(CV+PR) | (CV+PR+F+$CO_2$)-(CV+PR) |
| **5** | | | (CA+PG+F)-(CA+PG) | (CA+$CO_2$+PG)-(CA+PG) | (CA+PG+F+$CO_2$)-(CA+PG) |
| **6** | | | (CV+PG+F)-(CV+PG) | (CV+$CO_2$+PG)-(CV+PG) | (CV+PG+F+$CO_2$)-(CV+PG) |
| | **Effects** | | | | |
| | **A** | **B** | **C** | **D** | **E** |
| **1** | C (V-A)$_{\|PC}$ | P (R-C)$_{\|CA}$ | F$_{\|CA\ PC}$ | $CO_{2\|CA\ PC}$ | $CO_2$+F$_{\|CA\ PC}$ |
| **2** | C (V-A)$_{\|PR}$ | P (R-C)$_{\|CV}$ | F $_{\|CV\ PC}$ | $CO_{2\|CV\ PC}$ | $CO_2$+F$_{\|CV\ PC}$ |
| **3** | C (V-A)$_{\|PG}$ | P (G-C)$_{\|CA}$ | F $_{\|CA\ PR}$ | $CO_{2\|CA\ PR}$ | $CO_2$+F$_{\|CA\ PR}$ |
| **4** | | P (G-C)$_{\|CV}$ | F $_{\|CV\ PR}$ | $CO_{2\|CV\ PR}$ | $CO_2$+F$_{\|CVPR}$ |
| **5** | | | F $_{\|CA\ PG}$ | $CO_{2\|CA\ PG}$ | $CO_2$+F$_{\|CA\ PG}$ |
| **6** | | | F $_{\|CV\ PG}$ | $CO_{2\|CV\ PG}$ | $CO_2$+F$_{\|CV\ PG}$ |

### 2.2.4 Determination of the best model configuration

The performace of each model configuration to determine the Amazonia-Cerrado border was evaluated using two different metrics: The first metric is the correlation between total dry season LAI simulated by the model and the MODIS dry season LAI product in five longitudinal transects along the Amazon-Cerrado border, (described in Section 2.2.5). The second metric is correlation between simulated biomass and biomass data provided by Nogueira et al. (2014). The value of biomass was estimated by matching vegetation classes mapped at a scale of 1:250 000 and 29 biomass means from 41 published studies for vegetation types classified as forest (n=2317 plots) and as either non-forest or contact zones (1830 plots). For more details, see Nogueira et al. (2014).

### 2.2.5 Development of the MODIS LAI Map

The MODIS product used in this work is the MOD15A2, which is responsible for providing leaf area index data every 8 days, totalizing 46 images per year. When drawing up the MODIS LAI map, nine images per year were used, corresponding to the months of July, August and September, for the period of 2000-2008, amounting to 81 leaf area index images. These images were filtered by annual coverage maps and land use also provided by MODIS through the MOD12Q1 product in order to delete information from areas of non-natural vegetation. The filter was made considering a spatial resolution of 1 km.

The map of soil cover used uses a global land cover classification by The International Global Biosphere Programme (IGBP) (Belward et al., 1999; Friedl et al., 1999; Scepan, 1999) with 16 cover classes. The LAI information were filtered out for

the classes: cropland cover (12), urban and built-up (13), cropland/natural vegetation mosaics (14) and sparsely vegetated barrens (15). Then bi-linear interpolation to one-degree resolution was performed and the average of all images resulted on the average dry season leaf area index MODIS ($LAI_{dry}$), shown in Figure 7.

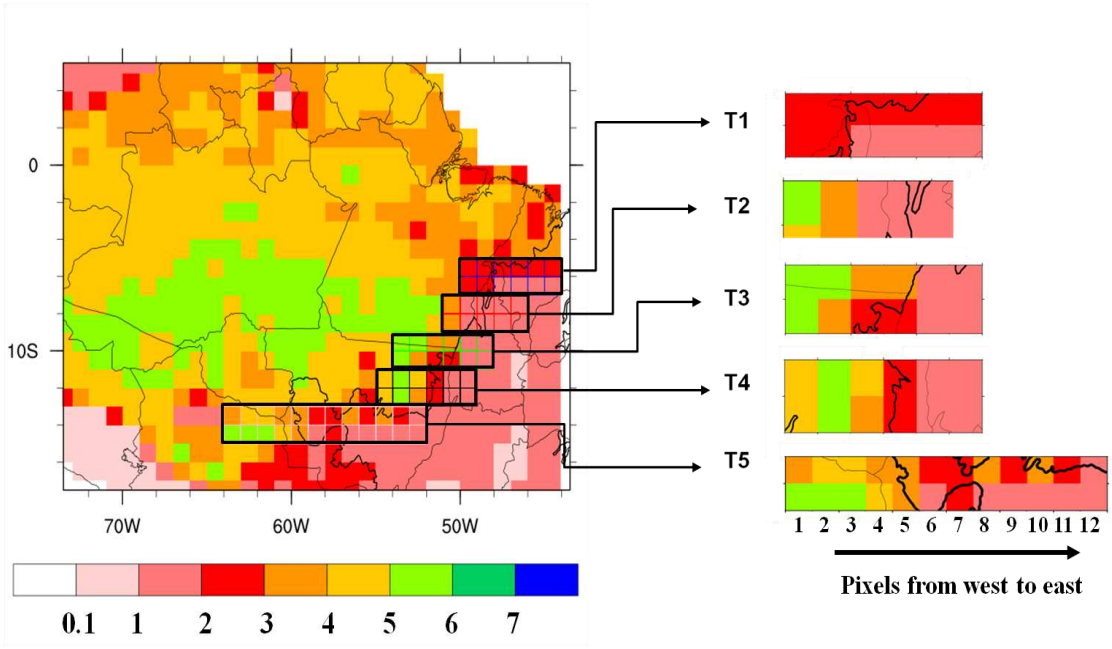


**Figure 7.** Map of the average dry season (July, August and September) leaf area index of MODIS product MOD15A2 from 2000 to 2008 and the five transects used in this study.

### 2.2.6 Statistical Analyses

The simulated variables were averaged for the last 10 years of simulation (1999-2008) and compared to $LAI_{dry}$ and biomass from Nogueira et al. (2014) within a grid cell. For statistical comparison we used the correlation coefficient and the Student t-test to verify a significant difference at $p<0.05$ of each of these variables for all of the simulated area.

## 2.3 RESULTS AND DISCUSSION

### 2.3.1 Comparison of simulations (Isolated Effects)

In this section we present the results of the isolated effects of climate, phosphorus, fire and $CO_2$ in the NPP, biomass and $LAI_{lower}$ and $LAI_{upper}$ canopies.

#### 2.3.1.1 Climate effects

Figure 8 shows the influence of the average climate (CA) and interannual variability (CV) on NPP, biomass, and $LAI_{upper}$ and $LAI_{lower}$.

For both climate conditions used (CA and CV), the INLAND represents well the Amazon-Cerrado transition (Figure 8a and 8b) with higher NPP values in the forest region and lower values in Cerrado.

NPP estimates from INLAND for the Amazon forest were compared against field data from LBA project and RAINFOR network sites (from KM67, ZF-2, UFAC, AGP, CAX, TAM and ZAR) described in Table 8.

INLAND simulated NPP values between 1.26 kg-C $m^{-2}$ $yr^{-1}$ and 0.94 kg-C $m^{-2}$ $yr^{-1}$ for Brazilian sites (KM67, ZF-2, UFAC, and CAX) and NPP values up to 1.42 kg-C $m^{-2}$ $yr^{-1}$ for the other sites. The differences between observed and simulated data for NPP in KM67 and ZF-2 were 9% in KM67 and 1% in ZF-2 when considering CA. When climate variability was considered the differences ranged between -4% and -24%. In other sites in the west Amazon basin such as AGP and ZAR (Colombia) NPP was overestimated in CA+PC (32% and 10%) and underestimated when CV was considered (-22% and -1%). UFAC and TAM, localized in the southwest Amazon basin, showed underestimates by INLAND when using CA (-5% and -7%) and overestimates when using CV (13.9% and 20.8%).

**Table 8.** NPP estimates from the INLAND and the relative errors for the KM67, ZF-2, UFAC, CAX, TAM, ZAR and AGP sites.

| Site | Period | Observed NPP | Average observed NPP | NPP INLAND | | Error % | Error % |
|---|---|---|---|---|---|---|---|
| | | | | CA+PC | CV+PC | CA+PC | CV+PC |
| KM67 | 2001 | 1.23 | 1.14 | 1.24 | 0.94 | 9 | -24 |
| | 2004 | 1.06 | | | | | -11 |
| ZF-2 | 2001 | 1.06 | 1.21 | 1.22 | 1.11 | 1 | 4 |
| | 2002 | 1.36 | | | | | -18 |
| UFAC | 2001 | 1.34 | 1.32 | 1.26 | 1.16 | -5 | -14 |
| | 2002 | 1.30 | | | | | -11 |
| CAX | 2004-2006 | 1.40 | 1.40 | 1.22 | 1.10 | -13 | -21 |
| TAM | 2005 | 1.53 | 1.53 | 1.42 | 1.27 | -7 | -17 |
| ZAR | 2004-2006 | 0.93 | 0.93 | 1.23 | 1.13 | 32 | 22 |
| AGP | 2004-2006 | 1.15 | 1.15 | 1.26 | 1.14 | 10 | -1 |

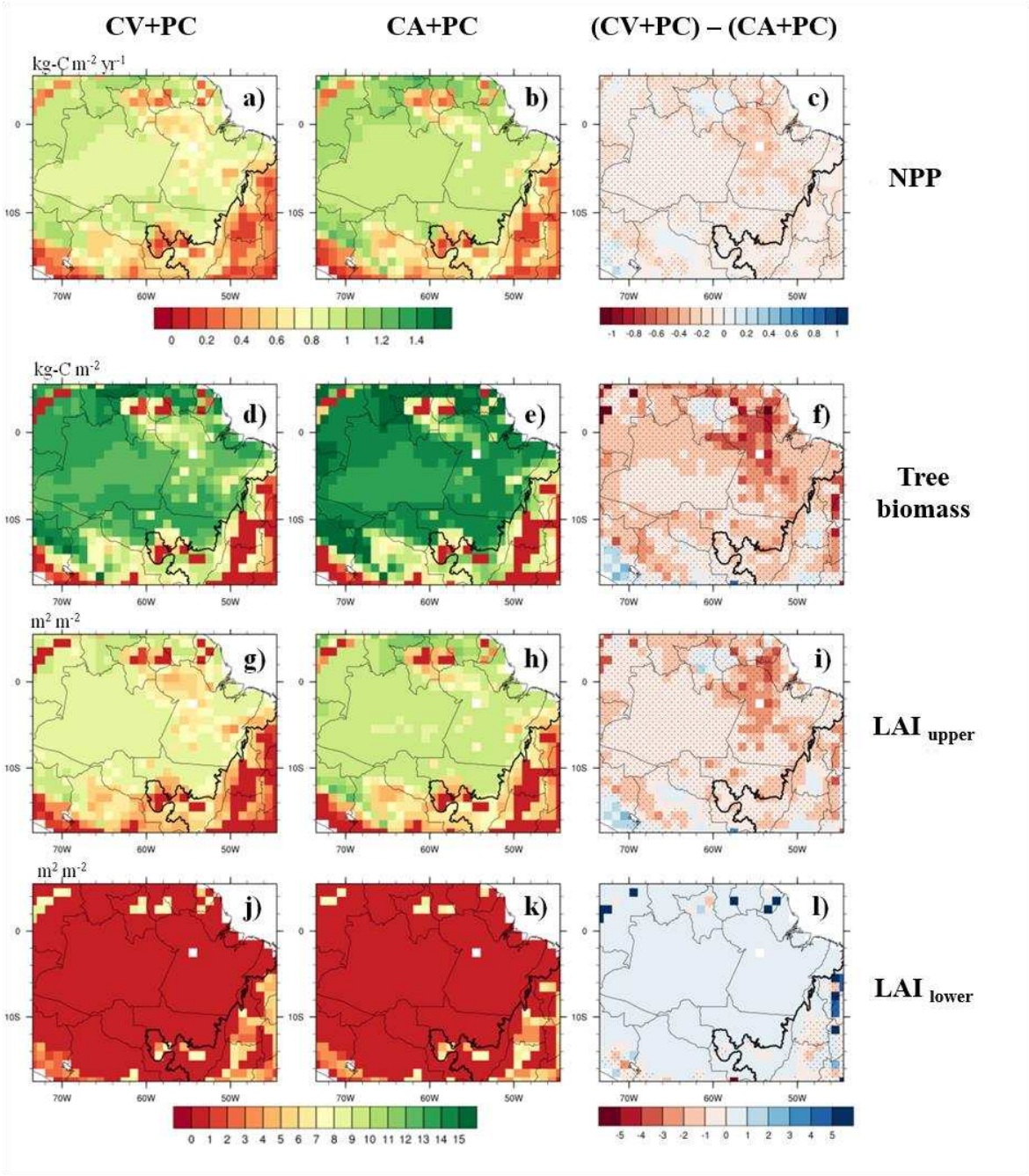


**Figure 8.** Climate variability effect on NPP, biomass, $LAI_{upper}$ and $LAI_{lower}$. The hatched areas indicate that the variables are statistically different compared to the control simulation at the level of 95% according to the t- test and the thick black line is the geographical limit of the Cerrado biome.

In the simulation under variable climate, NPP decreased between 0.2 and 0.4 kg-C $m^{-2}$ $yr^{-1}$ in biomes Amazonia and Cerrado and it was significantly different for the most part of the simulated area (Figure 8c). The values of NPP in Amazonia range

from 1.2 to 0.8 kg-C $m^{-2}$ $yr^{-1}$ with a northwest-southeast gradient in Amazonia, and in Cerrado range between 0.2 and 0.8 kg-C $m^{-2}$ $yr^{-1}$ (Figure 8). In percentage terms, NPP decreases 11% in the Amazon and 15% in the Cerrado, when the climate variability was considered.

The decrease in NPP is a consequence of the higher frequency of extreme precipitation, temperature and radiation associated with interanual climate variability, causing differences in the photosynthesis and annual carbon balance. In the Cerrado, the differences between CA and CV were higher because in this biome the seasonal variability of climate affects more intensely the vegetation, exposing the trees to soil water stress, decreasing the NPP more than in the Amazon region, where the seasonality of climate is less pronounced.

The small difference between total NPP values in CA and CV is probably related to the fact that there is offsetting between the $LAI_{upper}$ and $LAI_{lower}$, which causes the total carbon fluxes to vary little when only the climate varies (Figure 8). This result confirms the findings of Botta and Foley (2002), who found low sensitivity of total LAI and NPP simulated by the IBIS model to interannual climate variability. LAI is an important variable in the INLAND model because it is the main variable used to determine the dominant vegetation type that is assigned to a pixel. The simulated LAI follows the NPP gradient, with values ranging approximately from 5 to 11 $m^2$ $m^{-2}$ for $LAI_{upper}$ in the Amazon and 0 to 6 $m^2$ $m^{-2}$ in the Cerrado (Figure 8g and 8h). For $LAI_{lower}$ these values range between 0 and 6 $m^2$ $m^{-2}$ in Cerrado and close to zero in Amazonia (Figure 8j and 8k).

The high values of $LAI_{upper}$ and the low values of $LAI_{lower}$ clearly demonstrates the competition between trees and grasses in the model. In the forest-cerrado transition

it can be observed predominance of trees instead of grasses, except for the western region of the state of Mato Grosso, where higher $LAI_{lower}$ values can be observed (Figures 8j and 8k). In the central region of the Cerrado, a small area (along 45°W) with relatively high $LAI_{upper}$ values (Figures 8g and 8h) and low values $LAI_{lower}$ (Figures 8j and 8k) are found, featuring a forest in both climate scenarios.

The LAI simulated values are qualitatively representative, but they are probably overestimated. In the Amazon, LAI values generally vary from 4 to 8 $m^2\ m^{-2}$ (Carswell et al., 2002; McWilliam et al., 1993) and they are, in general, larger than the LAI observed in Cerrado. According to Miranda et al. (1997) and Hoffman et al. (2005), observed LAI in Cerrado range from below 1 to 2.5 $m^2\ m^{-2}$. In the Amazon region, the CV $LAI_{upper}$ decreased 11.9%, and 12.5% in the Cerrado with respect to the CA simulation, while for the $LAI_{lower}$, it increased 37% in the Amazon and 548% in Cerrado. The increase of 548% of $LAI_{lower}$ results from areas dominated by very low $LAI_{lower}$ values in CA (ie. areas between 10° S and -8° S in Cerrado domain, Figure 8k) and increased in CV to 6 - 7 $m^2\ m^{-2}$.

The biomass values in CV were between 7 and 15 kg-C $m^{-2}$ in the Amazon, and between 1 and 7 kg-C $m^{-2}$ in the Cerrado region (Figure 8). These values follow the same spatial gradient of the NPP and LAI, with higher values in the northwest and lower values in the southeast, with significant differences between the two simulation in the entire region. In the transition, the difference between CA and CV of the annual biomass resulted in a decline between 2 and 3 kg-C $m^{-2}$. The maximum decrease was in the Northern Amazonia (4 kg-C $m^{-2}$). In the Cerrado, some points were also influenced by this variability, reducing the upper canopy biomass by approximately 5 kg-C $m^{-2}$. In

the whole Amazon, when CV was used a reduction os arboreal biomass of 10.7% was found, while in the Cerrado, there was an increase of 5%.

#### 2.3.1.2 Phosphorus effect

The analysis of the phosphorus effect under variable climate indicates that the carbon assimilation was strongly limited by the phosphorus availability in the Amazon and the reduction in the NPP was significant for most of the Amazon area for both PR and PG datasets with respect to the PC control simulation (Figures 9 and 10). The decrease in NPP was approximately 0.2 and 0.4 kg-C $m^{-2}$ $yr^{-1}$ for PR and PG respectively, when compared to PC, except a few pixels in northeastern Amazonia where NPP decreased by more than 1 kg-C $m^{-2}$ $yr^{-1}$ for PG simulations.

In Cerrado, when PR was considered, the decreases in the NPP range from 0.1 to 0.2 kg-C $m^{-2}$ $yr^{-1}$ and were statistically different only in the new pixels added to the phosphorus regional dataset, as expected (Figure 9a).

In contrast, we found a small decrease in NPP for most of the Cerrado area when we considered PG. Although the decrease is not statistically significant, except for one pixel close to 52° W, it influences the decline on biomass in Cerrado (Figure 10b).

In INLAND, the NPP is directly affected by $V_{max}$, which is strictly dependent on soil phosphorus, and this relationship helps understand the results found. In the Amazon, the difference between the average $V_{max}$ (PG) and average $V_{max}$ (PR) was 0.06%. In the Cerrado, on the other hand, the magnitude $V_{max}$ (PG) is 75% of $V_{max}$ (PR), but the two simulations did not differ in mean stocks of biomass and NPP. This similarity between PR and PG may be due to the fact that representation of vegetation in

the INLAND model in this biome is dominated by grass, which is not influenced by P in the model.

The spatial variability of $LAI_{upper}$ (Figures 9c and Figure 10c) and biomass (Figures 9b and Figure 10b) for PR and PG reflect the spatial patterns of NPP along the Amazon-Cerrado transition.

The biomass decreased in the northwest of Amazonia and in the south (between Amazonas, Pará and northern of Mato Grosso states) from 2 to 5 kg-C $m^{-2}$ (Figure 9b) when PR was considered. The biomass gradient shows that the regional nutritional limitation is strongly influenced the boundary between Amazonia-Cerrado, following the trend of a more weathered area poor in soil P in the southeastern Amazon (Quesada et al., 2009).

On the other hand, when PG was used, a higher decrease in biomass was shown in Central Amazonia, in the northeast of Pará and in the northeast of Mato Grosso (Figure 10b), which agrees with the study of Mendes et al. (2013), which demonstrated that there is a close relationship between carbon assimilation and leaf phosphorus, in this region. Although the datasets have presented a different spatial gradient, both revealed that phosphorus limitation is higher in Amazonia than in the Cerrado.

The $LAI_{upper}$ follows a similar pattern of the biomass (Figures 9c and 10c), since the LAI values were determined from the produced leaf biomass and the leaf specific area for each PFTs in the model. The $LAI_{lower}$ from the simulated values of PR were not different from the simulation PC control in Cerrado, whereas the nutritional limitation map in PR did not include the Cerrado domain (Figure 9d).

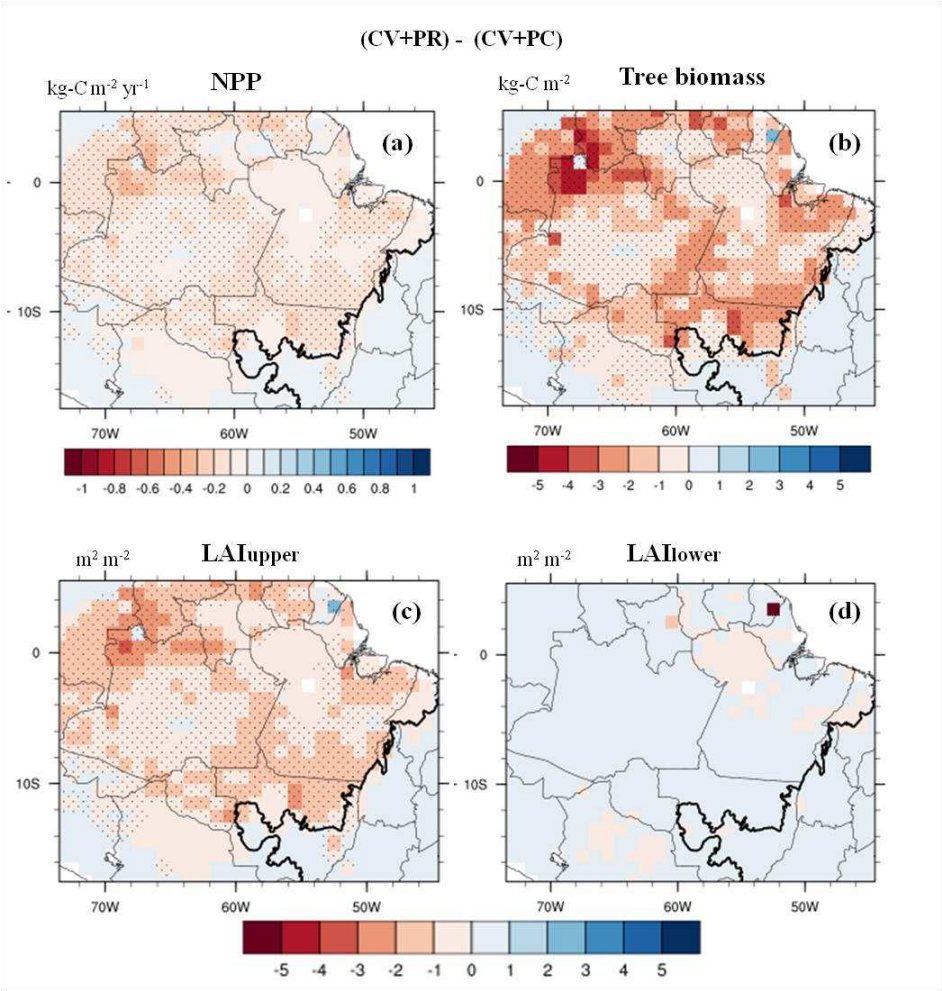


**Figure 9.** Regional Phosphorus effect (PR) on NPP (a); biomass (b); $LAI_{upper}$ (c); and $LAI_{lower}$ (d). The hatched areas indicate that the variables are significantly different compared to the control simulation at the level of 95% according to the t- test and the thick black line is the geographical limit of the Cerrado biome.

The small differences found in $LAI_{lower}$ between PG and PC (Figure 10d) could be due to the PG limited the photosynthetic rates of the arboreal component and it provided a small advantage of the water availability, favoring the increase of biomass and $LAI_{lower}$.

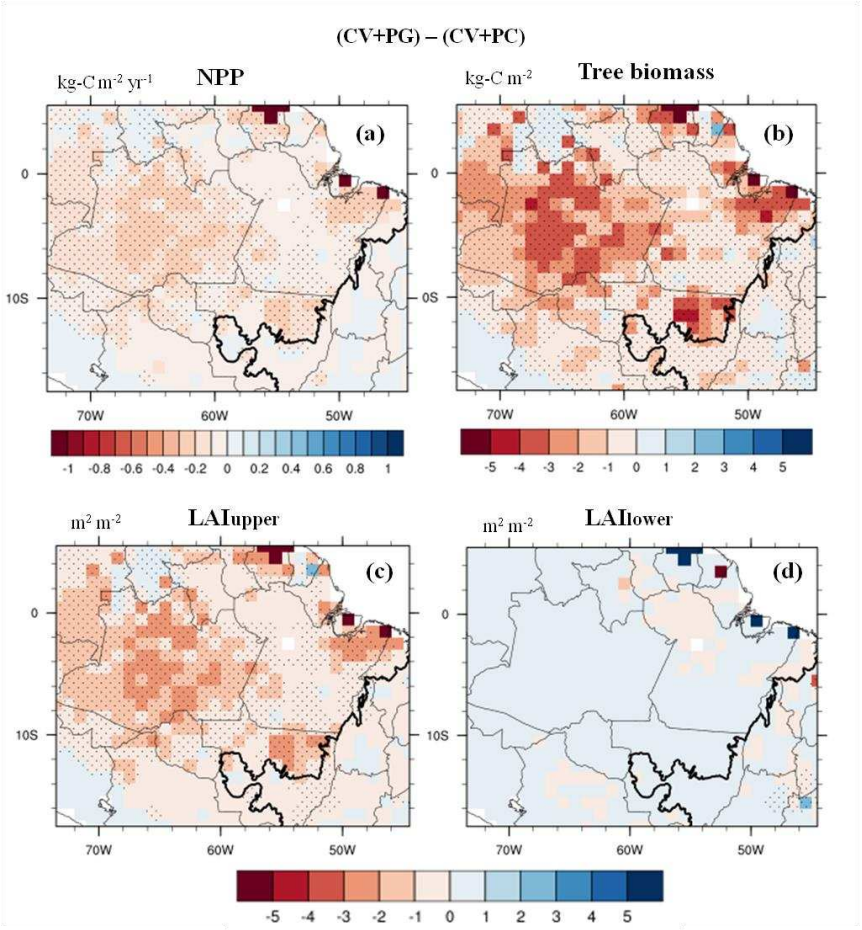


**Figure 10.** Global Phosphorus effect (PG) on NPP (a); biomass (b); $LAI_{upper}$ (c); and $LAI_{lower}$ (d). The hatched areas indicate that the variables are significantly different compared to the control simulation at the level of 95% according to the t- test and the thick black line is the geographical limit of the Cerrado biome.

### 2.3.1.3 Fire Effect

Overall, fire has an effect decreasing Cerrado biomass, decreasing upper canopy LAI and allowing the increase of the lower canopy LAI (Figure 11). Small parts of the dry forest also suffered the same effect, mainly in Rondonia, Bolivia and southern Peru.

The isolated effect of fire has similar behavior in CV simulations ($F_{|CV\ PC}$, $F_{|CV\ PR}$ and $F_{|CV\ PG}$) and strongly affected the biomass, $LAI_{upper}$ and $LAI_{upper}$ at the transition area (Figure 11). All these simulations resulted in decreases in biomass between 1 and 5 kg-C $m^{-2}$ along the transition, decreases in $LAI_{upper}$ between 2 and 4 $m^2\ m^{-2}$, and

increases in $LAI_{lower}$ between 1 and over 5 $m^2$ $m^{-2}$. In Mato Grosso state, where transition is longest the increase of $LAI_{lower}$ was above 4 $m^2$ $m^{-2}$ which indicates high fire activity.

In the Amazon, the small decrease of arboreal biomass in simulations reinforce the idea that the Amazon rainforest is naturally impervious to fire, contrary to the tropical savannas, which are naturally influenced by this disturbance (Lehmann et al., 2011; Murphy and Bowman, 2012). This influence of fire in tropical savannas has a great ecological importance and has been, for example, associated with the expansion of savannas in drier climate conditions as a major contributing factor (Couto-Santos et al., 2014; Silvério et al., 2013). Our results show that the fire effect in the Cerrado domain along the transition implies significant increases in $LAI_{lower}$, that represents shrubs and herbaceous vegetation (Figure 11g, Figure 11h, Figure 11i) and decreases significantly in $LAI_{upper}$ (Figure 11d, Figure 11e, Figure 11f), that represents trees, thus influencing the dynamics of upper and lower canopies. Under conditions of a future climate change scenario, this competition between trees and grasses can lead to a change in vegetation structure, favoring the expansion of grasses (Malhi et al., 2009).

In the Amazon domain along the transition it is evident that, although there was a significant decrease of the biomass (Figure 11a, Figure 11b, Figure 11c) in response to fire, the decrease in leaf area index was not of the same proportions (Figure 11d, Figure 11e, Figure 11f). This may be due to the much smaller time needed to build a leaf (< 1 year), when compared to the typical interval between disturbances in the forest region (several years).

The differences in the fire effects between the Amazon and Cerrado domains may be due the fact that the Amazon has denser forests and more humidity in

comparison to the Cerrado domain, and the latter is dominated by the presence of a continuous grassy layer that regains its flammability very quickly after burning. The Amazon is less flammable, generally burns less frequently and with less intensity, which allow this biome to maintain a dense canopy with distinct ecosystem properties (Eldridge et al., 2011). In the transition, the fire effects on $LAI_{upper}$ and $LAI_{lower}$ were inversely related. The decrease in the $LAI_{upper}$ led to an increase in radiation available to the lower canopy, which led to the spread of a shrub and herbaceous component. Therefore, there was a significant increase in $LAI_{lower}$, ranging up to 5 $m^2$ $m^{-2}$ in many places in the Cerrado.

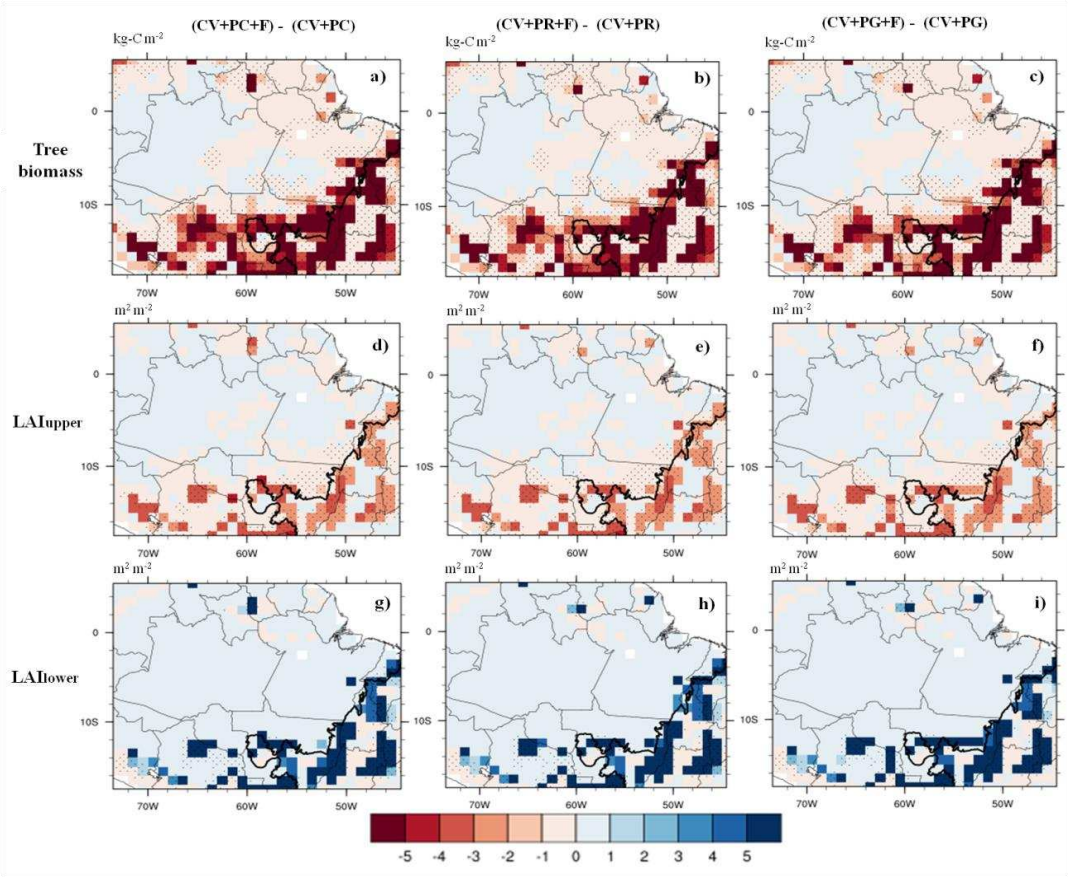


**Figure 11.** Fire effect on biomass, $LAI_{upper}$, and $LAI_{lower}$ for all soil phosphorus. The hatched areas indicate that the variables are significantly different compared to the control simulation at the level of 95% according to the t- test and the thick black line is the geographical limit of the Cerrado biome.

### 2.3.2 Longitudinal gradient of biomass and leaf area index in the Amazonia-Cerrado transition – Field observations

The five longitudinal transects used in the transition's analysis showed higher values in the west and lower values in the east for biomass (Nogueira et al., 2014) and dry season MODIS leaf area index ($LAI_{dry}$) (Figure 12). This gradient agrees with the trends observed by Malhi et al. (2006), who found higher biomass in the central Amazon compared to lower values in the southeast Amazon region. Observed data fields in the transition region are limited, and the existing data are estimates based on small samples, which reduces in part its reliability. On the other hand, remote sensing data such as MODIS are an alternative to large-scale studies because they provide good estimates of LAI, contributing to information on the dynamics and structure of vegetation.

In general, the MODIS $LAI_{dry}$ showed good correlation with the biomass data of Nogueira et al. (2014) for most transects analyzed, with correlation (R) values equal to 0.65 (transect 1 – T1), 0.74 (transect 2 – T2), 0.95 (transect 3 – T3), 0.89 (transect 4 – T4), and 0.54 (transect 5 – T5). The correlation between $LAI_{dry}$ and biomass was lower in the T1 and T5 than in transects located in the central transition. In T1 this may be due to higher precipitation levels in the region, allowing the maintenance of a forest with about the same LAI along the transect, although gradually changing to a less woody structure from west to east (Figure 12). The lowest correlation between the observed data was 0.54 for T5 which extends for 1332 km and has very heterogeneous vegetation crossing Pantanal, Amazonia and Cerrado. Biomass dataset in this transect presented high variability while $LAI_{dry}$ presented lower variability (Figure 12). The first four pixels of T5 are located outside of the map of biomass published by Nogueira et al.

(2014), and therefore were excluded from the correlation analysis. In the central Amazonia-Cerrado transition, the observed biomass and $LAI_{dry}$ MODIS showed better correlation with higher values (R). The data for all transects were used in the next Section (2.3.3) for comparison with INLAND model simulations.

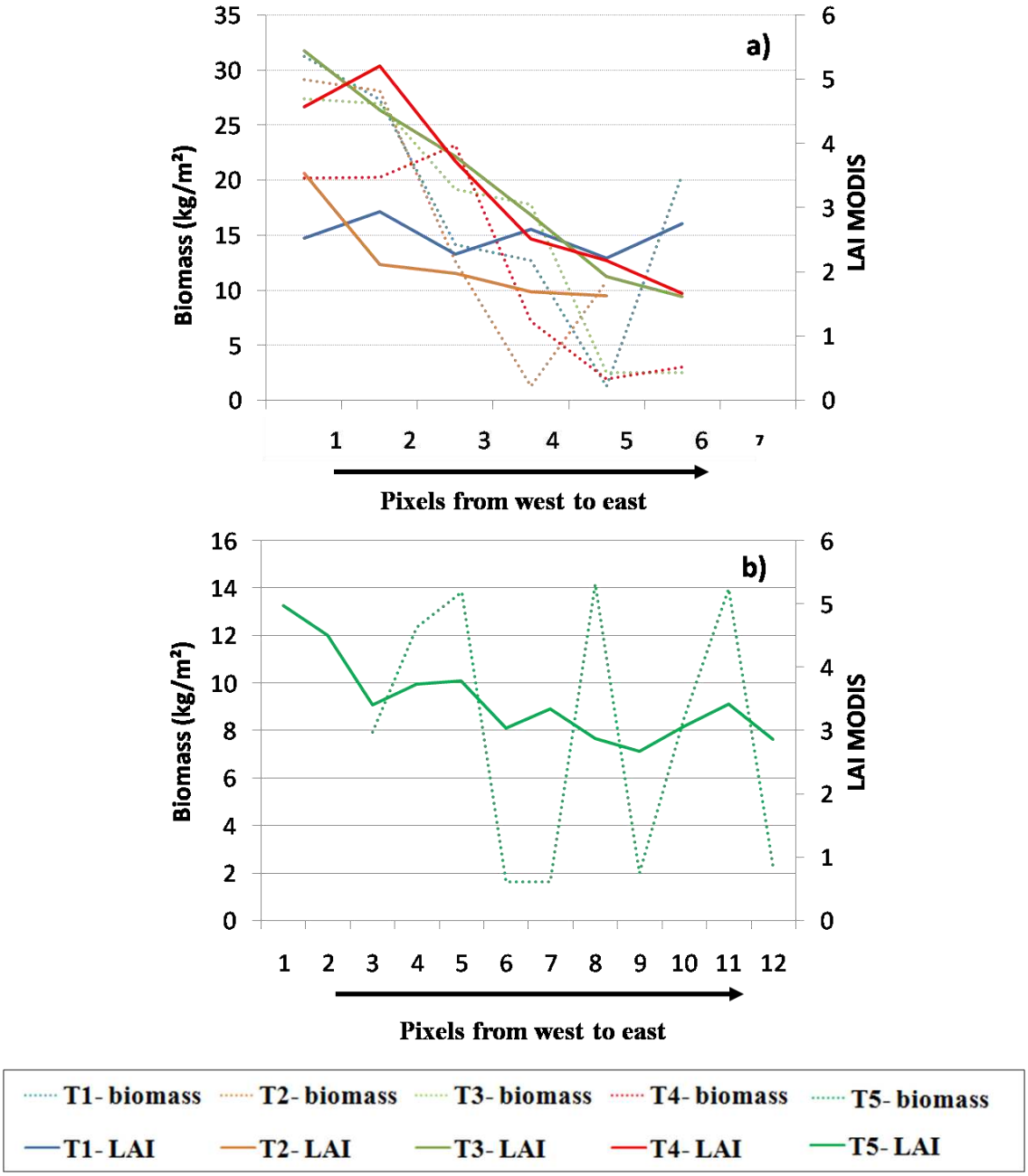


**Figure 12.** Longitudinal gradient of the dry season leaf area index ($LAI_{dry}$ – MODIS) and biomass (Nogueira et al., 2014) for the transects 1 to 4 (a) and transect 5 (b).

### 2.3.3 Longitudinal gradient of biomass and leaf area index in the Amazonia-Cerrado transition – Comparison between simulations and field observations

The comparison of simulated results considering the different combinations between nutritional limitation (PR and PG), occurrence of fire (F), interannual climate variability (CV) and average climate (CA) against the dry season LAI (MODIS- $LAI_{dry}$) and biomass data are presented in this Section.

All transects simulated show overestimated LAI (sum of $LAI_{upper}$ and $LAI_{lower}$) values and underestimation of biomass values (Appendix, Figures A1 and A2). Although the difference between simulated and observed values are not small, the INLAND model was able to adequately represent the longitudinal gradient for all transects, with higher values to the west and lower LAI and biomass values to the east. The correlations between simulated and observed values of LAI and biomass were higher when considering the interannual climate variability scenario (CV) for most transects, with average values of 0.49 for LAI and 0.71 for biomass (Tables 9 and 10).

**Table 9.** Correlation coefficients of dry season LAI simulated by INLAND and remote sensing estimates by MODIS.

| | **T1** | | **T2** | | **T3** | | **T4** | | **T5** | | **Transects average** | |
|---|---|---|---|---|---|---|---|---|---|---|---|---|
| | CA | CV | CA | CV | CA | CV | CA | CV | CA | CV | CA | CV |
| PC | 0.25 | 0.25 | 0.47 | 0.45 | 0.85 | 0.91 | 0.80 | 0.84 | 0.39 | 0.39 | 0.55 | 0.57 |
| PR | 0.22 | 0.22 | 0.43 | 0.39 | 0.83 | 0.89 | 0.81 | 0.29 | 0.42 | 0.49 | 0.54 | 0.46 |
| PG | 0.26 | 0.26 | 0.55 | 0.52 | 0.78 | 0.84 | 0.75 | 0.78 | 0.53 | 0.59 | 0.58 | 0.60 |
| PC+F | 0.32 | 0.14 | 0.44 | 0.38 | 0.71 | 0.92 | 0.72 | 0.84 | 0.28 | 0.19 | 0.50 | 0.49 |
| PR+F | 0.30 | 0.22 | 0.39 | 0.20 | 0.57 | 0.78 | 0.47 | 0.62 | 0.25 | 0.24 | 0.40 | 0.41 |
| PG+F | 0.34 | 0.10 | 0.50 | 0.44 | 0.48 | 0.79 | 0.36 | 0.81 | 0.35 | 0.35 | 0.41 | 0.50 |
| PC+F+$CO_2$ | 0.18 | 0.17 | 0.43 | 0.39 | 0.72 | 0.91 | 0.70 | 0.83 | -0.06 | 0.06 | 0.39 | 0.47 |
| PR+F+$CO_2$ | 0.38 | 0.21 | 0.31 | 0.33 | 0.41 | 0.74 | 0.69 | 0.79 | -0.07 | 0.08 | 0.34 | 0.43 |
| PG+F+$CO_2$ | 0.40 | 0.24 | 0.45 | 0.37 | 0.52 | 0.71 | 0.60 | 0.80 | 0.03 | 0.20 | 0.40 | 0.46 |
| Average | 0.29 | 0.20 | 0.44 | 0.39 | 0.65 | 0.83 | 0.66 | 0.73 | 0.24 | 0.29 | 0.46 | 0.49 |

**Table 10.** Correlation coefficients of biomass simulated by INLAND and field estimates biomass (Nogueira et al., 2014).

| | **T1** | | **T2** | | **T3** | | **T4** | | **T5** | | **Transects average** | |
|---|---|---|---|---|---|---|---|---|---|---|---|---|
| | CA | CV | CA | CV | CA | CV | CA | CV | CA | CV | CA | CV |
| PC | 0.88 | 0.83 | 0.56 | 0.53 | 0.84 | 0.87 | 0.79 | 0.80 | 0.26 | 0.30 | 0.67 | 0.66 |
| PR | 0.87 | 0.82 | 0.42 | 0.39 | 0.82 | 0.84 | 0.78 | 0.78 | 0.34 | 0.41 | 0.65 | 0.65 |
| PG | 0.87 | 0.82 | 0.57 | 0.54 | 0.79 | 0.81 | 0.71 | 0.71 | 0.39 | 0.44 | 0.67 | 0.66 |
| PC+F | 0.76 | 0.80 | 0.93 | 0.91 | 0.90 | 0.91 | 0.73 | 0.71 | 0.12 | 0.35 | 0.69 | 0.74 |
| PR+F | 0.72 | 0.76 | 0.92 | 0.91 | 0.90 | 0.92 | 0.75 | 0.74 | 0.12 | 0.35 | 0.69 | 0.74 |
| PG+F | 0.71 | 0.80 | 0.93 | 0.92 | 0.91 | 0.93 | 0.64 | 0.72 | 0.15 | 0.39 | 0.67 | 0.75 |
| PC+F+$CO_2$ | 0.78 | 0.80 | 0.93 | 0.91 | 0.84 | 0.92 | 0.78 | 0.73 | 0.23 | 0.33 | 0.71 | 0.74 |
| PR+F+$CO_2$ | 0.66 | 0.77 | 0.90 | 0.89 | 0.95 | 0.85 | 0.74 | 0.73 | 0.35 | 0.34 | 0.72 | 0.72 |
| PG+F+$CO_2$ | 0.63 | 0.76 | 0.91 | 0.91 | 0.91 | 0.94 | 0.54 | 0.72 | 0.21 | 0.34 | 0.64 | 0.74 |
| Average | 0.76 | 0.80 | 0.79 | 0.77 | 0.87 | 0.89 | 0.72 | 0.74 | 0.24 | 0.36 | 0.68 | 0.71 |

The LAI correlation considering only nutritional limitation was higher in PG (0.60) than when using regional phosphorus (PR, 0.46) in the average of the transects (Table 9). Also in the biomass comparison (Table 10), the simulated data showed higher correlation with the observed data in PG (0.66) was in PR (0.65), reinforcing that the use of PG represented the observed data better than PR.

When incorporating the effect of fire (PC+F; PR+F; PG+F), it is possible to observe a decrease in correlations for LAI (Table 9) and an increase in correlations for biomass (Table 10) for all nutritional scenarios. With the fire effect, the best correlations were PG+F with 0.50 for LAI and 0.75 for biomass.

On average for all transects, the combined effect of nutritional limitation, fire and $CO_2$ for LAI showed higher correlation for PC+F+$CO_2$ (0.47) than for PR+F+$CO_2$ (0.43) and for PG+F+$CO_2$ (0.46) (Table 9). PC+F+$CO_2$ and PG+F+$CO_2$ have similar correlations (0.74) for biomass (Table 10). The addition of the transient $CO_2$ factors to simulations decreased correlations for LAI and biomass, in relation to considering only fire and nutritional limitations.

The average correlations for LAI at transects T1 and T2 – northern part of the transition area – were, respectively, 0.20 and 0.39, that are considered low. On the other hand, the average correlations for biomass in these transects were considered high, 0.80 and 0.77 for respectively T1 and T2. This difference suggests possible distortions in $LAI_{dry}$ values, once a high correlation was found for the biomass. It is known that the products of the MODIS sensor in higher rainfall regions are influenced by cloudiness, which affects the accuracy and robustness of the information collected on these regions. The average LAI values used, however, corresponds to months of lower precipitation and cloudiness, which minimizes this potential interference. On the other hand, it is possible that the lower correlations are due to low variations of the simulated LAI values by the INLAND model between the rainy and dry months. The carbon increase in the leaves is controlled by the model's vegetation dynamics module that adjusts the LAI values annually. Possibly, this module may not change in appropriate proportions the LAI in these areas.

The T3 and T4 transects located in the central region of the Amazon-Cerrado transition showed high average correlations between observed and simulated data for both variables, LAI and biomass, when CV were considered (Table 9 and Table 10). The average correlation values for LAI were 0.83 for T3 and 0.73 for T4, and for biomass were 0.89 for T3 and 0.74 for T4, showing high affinity between simulated and observed values. In these regions, that show greater amplitude of the precipitation annual cycle, the model was better suited to simulate variations of LAI, NPP and biomass values. In regions with lower amplitude and variation in annual precipitation, lower average correlations were found. This suggests that the model did not capture the real variation of LAI because it did not seasonally change the rate of photosynthesis

enough to affect the feedback system – similar to that previously discussed for the transect T1 and T2. The T5 transect, located south of the transition, presented low average correlations for CV and CA. This region, characterized by broad vegetation heterogeneity, makes not only the representation through simulation difficult, but also the collection of large-scale data for validation.

In general, the INLAND model simulations showed high and positive correlations, mainly for transects located in the central region of the Amazon-Cerrado transition. This relationship between the observed data and simulated values was stronger when considering the interannual climate variability, especially for biomass, i.e., the use of an average climate decreases the accuracy of the model in simulating the NPP dynamics, biomass, and consequently LAI.

The highest correlation found, however, was for biomass in PG+F+$CO_2$ in the transect T3 where the correlation coefficient was equal to 0.94. This high correlation to biomass was accompanied by a correlation of 0.71 for LAI, the lowest in T3.

The low correlation in PG+F+$CO_2$ for LAI in T3 may be connected to the fact that the fire effect on the LAI is, in some ways, a compensatory effect in the INLAND model. It happens because the LAI reduction in the arboreal vegetation implies an increase in the LAI for grasses, which means the model will always have high levels of total LAI. These high LAI values do not necessarily imply a high biomass once LAI can increase quickly after the fire occurrence, which may explain the higher correlations for biomass when compared to LAI.

The correlations between the simulated and observed biomass were better than the correlations between simulated and observed LAI. It means that, while the model is

able to capture the Amazon-Cerrado gradient, this robustness is more due to the estimate of biomass than of LAI.

### 2.3.4 Simulated composition of vegetation

INLAND describes the structure and composition of vegetation communities based on different plant functional types (e.g., tropical broadleaf evergreen trees or C4 grasses). The model has a dynamic vegetation module and, if this module is used, the vegetation type that dominates a particular region can change dynamically to another based on LAI. The model specifies that tropical evergreen forest and tropical deciduous forest ecosystems are characterized by $LAI_{upper}$ above 2.5 $m^2$ $m^{-2}$. $LAI_{upper}$ values between 0.8 and 2.5 $m^2$ $m^{-2}$ characterize savannas, and values smaller than 0.8 $m^2$ $m^{-2}$ characterize grassland ecosystems.

The previous results showed that biomass is simulated more robustly than the LAI. However, this robustness appears to be more quantitative than qualitative, since the model was able to capture the Amazon-Cerrado gradient with higher LAI values in the west and lower values in the east (Figure 12). The LAI estimated by INLAND for the Amazon was between 7.5 and 11 $m^2$ $m^{-2}$, and 0 - 6 $m^2$ $m^{-2}$ for Cerrado (Figure 8). These values are overestimated when compared with MODIS observations, these being respectively between 4 and 7 $m^2$ $m^{-2}$ for Amazonia, and 0 and 3 $m^2$ $m^{-2}$ for Cerrado (Figure 7).

Although the simulated LAI was overestimated when compared with MODIS observations, it represents well the distribution of vegetation in some conditions with fire and nutritional limitation (Figures 13 and 14). We evaluated the INLAND ability to assign the type of dominant vegetation analyzing 10 years of probability of occurrence.

If the dominant vegetation type in a pixel is identical in greater than 90% of the simulated years (9 of 10), then the simulated vegetation is defined as “very robust” for that pixel; if it occurs in 70 - 90% of the simulated years, it is considered to be “robust”. If the dominant vegetation occurred in less than 70% of simulated years, the pixel considered “transitional” vegetation (Figures 13 and 14).

Most of the pixels showed agreement above 90% in vegetation cover classification for CA (Figures 13b, 13d and 13f). A larger number of pixels with values below 70% agreement was observed when considering CV compared to CA. This increase in the heterogeneity of the pixels is due to a higher variation of annual carbon flux induced by the interannual climate variability that directly affects the LAI.

In addition to the overall decrease in robustness, we observed a higher variability in CV compared to CA simulations when we added different effects (P, F or $CO_2$). Probably, the effect of these factors associated with climate variability acted more strongly on the plants’ physiological processes and directly affected the NPP, biomass and LAI. The composition of the vegetation in all nutritional limitation only scenarios for CA simulations resulted in >90% of agreement on the vegetation type for nearly all pixels (Figures 13b, 13d and 13f). CA+PC and CA+PR simulations had the same composition of the vegetation, while CA+PG replaced the deciduous forest by evergreen forest in the central Cerrado region, around 8° S 46° W (Figures 13a, 13c and 13e). Cerrado was better represented in CV+PC, CV+PR and CV+PG than in the same CA combinations (Figures 14a, 14c and 14e). The occurrence of forested areas in the central Cerrado decreased in CV+PC, these being replaced by the savanna vegetation class (Figures 14a, 14c and 14e). However, some areas of perennial forest remained in the central Cerrado in CV+PG, as in CA+PG (Figure 14e).

When the effect of fire was added to CA simulations, we can observe an increase in uncertainty on the vegetation cover classification in the Cerrado region. The effect of fire reduced the presence of deciduous forest in central Cerrado biome when compared to PC and PC+$CO_2$, and the vegetation was replaced by evergreen forest and savanna (Figures 13m, 13o and 13q). In CV simulations, the fire effect results in the replacement of the deciduous and perennial forest by savanna and grasses in all Cerrado central region (Figures 14m, 14o and 14q). This replacement indicated an improvement in the representation of vegetation classes in the Amazon-Cerrado transition.

Few changes in the vegetation composition due to the $CO_2$ influence were found in the border region when both climate scenarios were compared with the control simulation. However, the $CO_2$ changed vegetation classes in some locations in the central Cerrado. The major portion of the deciduous forest in CA+PC and CA+PR (Figures 13g and 13i) was transformed in evergreen forest and savanna in CA+PC+$CO_2$ and CA+PR+$CO_2$ (Figures 14g, and 14i). The differences between CA+PG+$CO_2$ and CV+PG+$CO_2$ are smaller but can be noted in the central Cerrado region.

Finally, we analyzed the effects of the combinations of nutritional limitation, fire and $CO_2$ on vegetation. The Amazon transition vegetation was better represented in CV and the border of the majority of the savanna class roughly matched the Amazon-Cerrado border set by PROBIO in this simulation (Figure 14x). This combination also results in savanna and grasses dominating the central Cerrado. Althought INLAND model overestimated LAI values, this model can represent well the distribution and classification of the Amazon-Cerrado transition under the effects of nutritional limitation, fire and $CO_2$ when climate variability is considered. This improvement can

be confirmed not only by visual analysis of the vegetation composition, but also through improvements in the correlations when considering CV.

Although the model has performed well in representing the composition of the vegetation in all cases, no changes were found for the southern region of Mato Grosso state. There is one small area of evergreen forest, suggesting that this region may have soil physical and chemical properties different from those used in the model. In the northern Amazon, INLAND could represent with >90% robustness the Cerrado areas in all simulations.

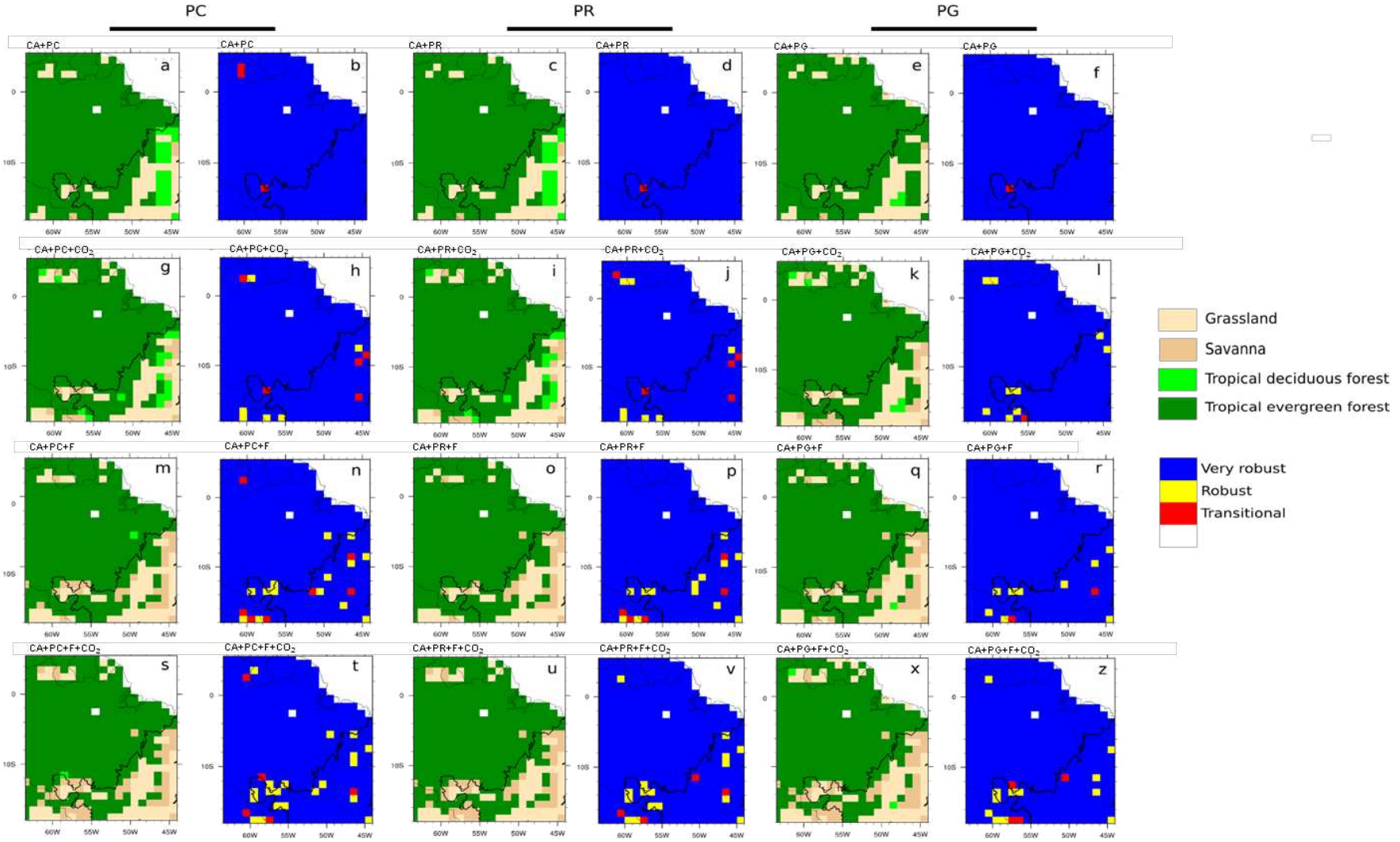


**Figure 13.** Results of the vegetation composition when incorporated the effects of nutritional limitation, fire and $CO_2$ in CA and simulated pattern of dominant vegetation.

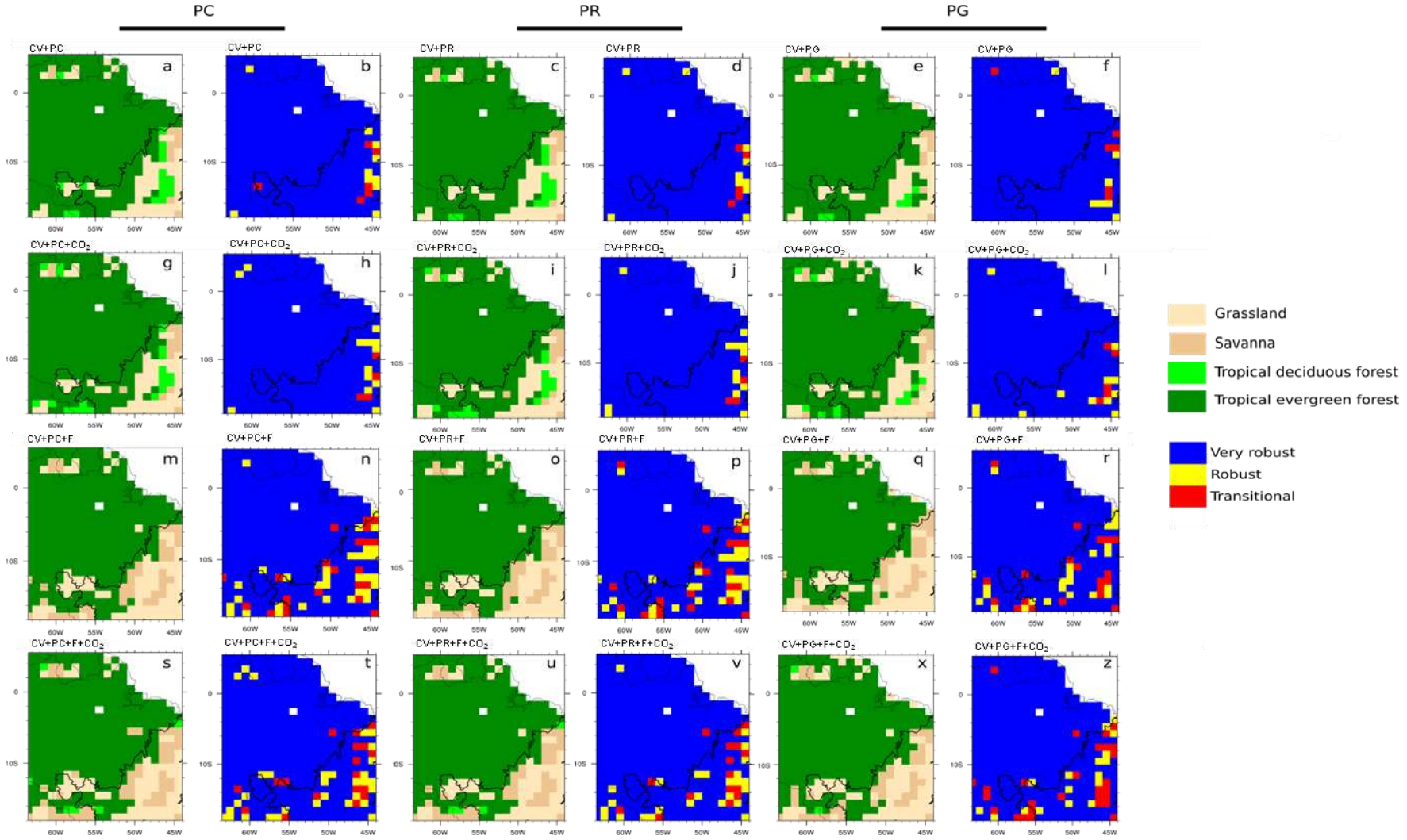


**Figure 14.** Results of the vegetation composition when incorporated the effects of nutritional limitation, fire and $CO_2$ in CV and simulated pattern of dominant vegetation.

## 2.4 CONCLUSIONS

Results from the model simulations indicate that, in INLAND, climate variability and interannual disturbances such as fire have a major impact on the vegetation structure. Processes of competition between trees and grasses for resources are intensified, changing the vegetation cover with little variation in carbon storage.

The experiments conducted to evaluate the effect of nutritional limitation on vegetation in the Amazon-Cerrado transition revealed that phosphorus is more limiting in the Amazon than in the Cerrado, highlighting the importance of incorporating P dynamics in DGVMs, since tropical forests have a determinant role in the global carbon balance. In the Cerrado, on the other hand, the effect of nutritional limitation is smaller but not insignificant, since our correlations showed an improvement in correlation between predicted and observed data for LAI and biomass in the presence of phosphorus limitations.

In the Cerrado region, the effect of fire is much more intense than the effects of the nutritional limitation, so that in the transition region fire can be considered the main agent of change in the vegetation. Fire effects on the structure and dynamics of vegetation are directly linked to their intensity and frequency, which commonly results from a more humid or drier climate. When evaluated in combination with $CO_2$, the effects of nutritional restriction and fire showed fewer changes in land cover, so its addition brought complexity and nonlinearity to the results.

Although our results have identified a better representation of biomass by the INLAND model compared to LAI, significant improvements in the representation of the Amazon-Cerrado border were found when the effects of phosphorus and fire were considered. The addition of nutritional limitation, fire, and subsequently $CO_2$, gradually improved representation of the

Amazon-Cerrado LAI gradient, causing the model to simulate the current position of biomes. The best combination for representing the Amazon-Cerrado border was the CV+PG+F+$CO_2$ scenario.

## 3. GENERAL CONCLUSIONS

In general, we conclude that climate, fire and soil phosphorus have an important role in the dynamics of vegetation along the Amazon-Cerrado transition, changing the net primary productivity, biomass and leaf area index. Although these factors are important, and of great interest for community scientific, the lack of observed data in transition regions is still a major limitation for the improvement of the dynamic global vegetation models. In this work we had difficulty obtaining observed data for physiological parameters such as soil P and $V_{max}$, for the Amazonia-Cerrado transition, because most of the available observed data for physiological parameters refers to a particular type of vegetation or predominant species, not representing the transition area.

Given this limitation, we use a pre-established relationship between $V_{max}$ and total soil phosphorus total ($P_{total}$) to estimate $V_{max}$, remote sensing data to obtain LAI and a biomass map. However, finding soil phosphorus total measurements was also a challenge. Most soil phosphorus data does not follow a common protocol, ie, there are measurements of the available phosphorus in the soil obtained from different extractors, making it difficult to compare and use of this data together. In addition, most of the information about the soil phosphorus content is not accompanied by data as texture, clay content, soil type, which makes it even more complex the use of this information. To solve part of this problem and homogenise the soil data measurements used, we used a mathematical model to estimate the soil phosphorus total from phosphorus values obtained by Mehlich-1 extractor. This effort allowed the development of a phosphorus regional map in the Amazon-Cerrado transition incorporating phosphorus data collected in the Mato Grosso state and the allowing a numerical experiment with the INLAND model.

From the numerical experiment, it is possible to conclude that the use of climate interannual variability resulted in a statistically significant decrease of carbon increment and improved the correlation between observed and simulated LAI and biomass. Fire showed a statistically significant influence only in the Amazon-Cerrado border, not affecting Central Amazonia. The effects of nutritional limitation were more important in the Amazon than in the Cerrado biome.

When used in combination, however, these factors improved the spatial representation of vegetation classes in the model. These results showed that the INLAND model can be a powerful tool in assessing possible changes in vegetation under scenarios of future climate change and emphasize the importance of a greater number of observed data. To further study the nutritional limitation in transition areas, it is recommended to use Hedley fractionation data obtained for total soil phosphorus, because this method also allows the extraction of more varied forms of available phosphorus in the soil, which can help us to quantify how much of the total phosphorus acts in the nutritional limitation of photosynthesis.

Suggestions for future implementations in INLAND include: a) modifications in the INLAND phenology module improve the representation of the seasonal LAI; b) substitution of the prescribed C:N ratio existing the model by a dynamic soil N cycle, since the phosphorus photosynthesis limitation depends on the nitrogen content in the leaves; and finally c) implementation of a dynamic phosphorus cycle and nonlinear interactions between the phosphorus present in the leaves and soil.

## 4. REFERENCES

Alves, D. S., Soares, J. V., Amaral, S., Mello, E. M. K., Almeida, S. A. S., Da Silva, O. F. and Silveira, A. M.: Biomass of primary and secondary vegetation in Rondônia, Western Brazilian Amazon, **Glob. Chang. Biol.**, 3, 451–461, doi:10.1046/j.1365-2486.1997.00081.x, 1997.

Alves, M. E. and Lavorenti, A.: Remaining phosphorus estimate through multiple regression analysis, **Pedosphere**, 16(5): 566-571, 2006.

Amthor, J. S.: The role of maintenance respiration in plant growth, **Plant, Cell Environ**., 7, 561–569, doi:10.1111/j.1365-3040.1984.tb01856.x, 1984.

Aragão, L. E. O. C., Malhi, Y., Metcalfe, D. B., Silva-Espejo, J. E., Jiménez, E., Navarrete, D., Almeida, S., Costa, A. C. L., Salinas, N., Phillips, O. L., Anderson, L. O., Baker, T. R., Goncalvez, P. H., Huamán-Ovalle, J., Mamani-Solórzano, M., Meir, P., Monteagudo, A., Peñuela, M. C., Prieto, A., Quesada, C. A., Rozas-Dávila, A., Rudas, A., Silva Junior, J. A. and Vásquez, R.: Above and below-ground net primary productivity across ten Amazonian forests on contrasting soils, **Biogeosciences Discuss.**, 6, 2441–2488, doi:10.5194/bgd-6-2441-2009, 2009.

Arora, V. K. and Boer, G. J.: A parameterization of leaf phenology for the terrestrial ecosystem component of climate models, **Glob. Chang. Biol.**, 11, 39–59, doi:10.1111/j.1365-2486.2004.00890.x, 2005.

Bahia Filho, A. F. C.: **Índices de disponibilidade de fósforo em latossolos do Planalto Central com diferentes características texturais e mineralógicas**, Tese (Doutorado em Solos e Nutrição de Plantas) – Viçosa – MG, Universidade Federal de Viçosa – UFV, 178p. 1982.

Belward, A. S., Estes, J. E. and Kline, K. D.: The IGBP-DIS Global 1-km Land-Cover Data Set DISCover: A Project Overview, **Photogramm. Eng. Remote Sensing**, 65, 1013–1020, 1999.

Betts, R. A., Cox, P. M., Collins, M., Harris, P. P., Huntingford, C. and Jones, C. D.: The role of ecosystem-atmosphere interactions in simulated Amazonian precipitation decrease and forest dieback under global climate warming, **Theor. Appl. Climatol.**, 78, 157–175, doi:10.1007/s00704-004-0050-y, 2004.

Bloomfield, K. J., Domingues, T. F., Saiz, G., Bird, M. I., Crayn, D. M., Ford, A., Metcalfe, D. J., Farquhar, G. D. and Lloyd, J.: Contrasting photosynthetic characteristics of forest - savanna species (Far North Queensland, Australia), **Biogeosciences**, (11), 7331–7347, doi:10.5194/bg-11-7331-2014, 2014.

Bognola, I. A.: **Caracterização química, física e mineralógica de solos intermediários entre Latossolos Brunos e Latossolos Roxos**, Tese (Mestrado em Solos e Nutrição de Plantas) – Viçosa – MG, Universidade Federal de Viçosa – UFV, 205p. 1995.

Botta, A. and Foley, J. A.: Effects of climate variability and disturbances on the Amazonian terrestrial ecosystems dynamics, **Global Biogeochem. Cycles**, 16(4), doi:10.1029/2000GB001338, 2002.

Campello, M. R., Novais, R. F., Fernandez, R. I. E., Fontes, M. P. F. and Barros, N. F.: Avaliação da reversibilidade de fósforo não-lábil para lábil em solos com diferentes características, **Rev. Bras. Ciência do Solo**, 18, 157–165, 1994.

Carswell, F. E., Costa, A. L., Palheta, M., Malhi, Y., Meir, P., Costa, J. D. P. R., Ruivo, M. D. L., Leal, L. D. S. M., Costa, J. M. N., Clement, R. J. and Grace, J.: Seasonality in $CO_2$ and $H_2O$ flux at an eastern Amazonian rain forest, **J. Geophys. Res. D Atmos.**, 107, doi:10.1029/2000JD000284, 2002.

Castanho, A. D. A., Coe, M. T., Costa, M. H., Malhi, Y., Galbraith, D. and Quesada, C. A.: Improving simulated Amazon forest biomass and productivity by including spatial variation in biophysical parameters, **Biogeosciences**, 10(4), 2255–2272, doi:10.5194/bg-10-2255-2013, 2013.

Couto-Santos, F. R., Luizão, F. J. and Carneiro Filho, A.: The influence of the conservation status and changes in the rainfall regime on forest-savanna mosaic dynamics in Northern Brazilian Amazonia, **Acta Amaz.**, 44(2), 197–206, 2014.

Cox, P. M., Betts, R. A., Collins, M., Harris, P. P., Huntingford, C. and Jones, C. D.: Amazonian forest dieback under climate-carbon cycle projections for the 21st century, **Theor. Appl. Climatol.**, 78, 137–156, doi:10.1007/s00704-004-0049-4, 2004.

Cross, A. F. and Schlesinger, W. H.: A literature review and evaluation of the Hedley fractionation: Applications to the biogeochemical cycle of soil phosphorus in natural ecosystems, **Geoderma**, 64, 197–214, doi:10.1016/0016-7061(94)00023-4, 1995.

Davidson, E. A., Reis de Carvalho, C. J., Vieira, I. C. G., Figueiredo, R. D. O., Moutinho, P., Yoko Ishida, F., Primo dos Santos, M. T., Benito Guerrero, J., Kalif, K. and Tuma Sabá, R.: Nitrogen and Phosphorus Limitation of Biomass Growth in a Tropical Secondary Forest, **Ecol. Appl.**, 14(4), 150–163, doi:10.1890/01-6006, 2004.

Domingues, T. F., Meir, P., Feldpausch, T. R., Saiz, G., Veenendaal, E. M., Schrodt, F., Bird, M., Djagbletey, G., Hien, F., Compaore, H., Diallo, A., Grace, J. and Lloyd, J.: Co-limitation of photosynthetic capacity by nitrogen and phosphorus in West Africa woodlands, **Plant, Cell Environ.**, 33, 959–980, doi:10.1111/j.1365-3040.2010.02119.x, 2010.

Eldridge, D. J., Bowker, M. A., Maestre, F. T., Roger, E., Reynolds, J. F. and Whitford, W. G.: Impacts of shrub encroachment on ecosystem structure and functioning: Towards a global synthesis, **Ecol. Lett.**, 14, 709–722, doi:10.1111/j.1461-0248.2011.01630.x, 2011.

Fabres, A. S.: **Disponibilidade de fósforo em solos e concentrações críticas de diferentes frações de fósforo em plantas de alface cultivadas em amostras de diferentes solos**, Tese (Mestrado em Solos e Nutrição de Plantas) – Viçosa – MG, Universidade Federal de Viçosa – UFV, 36p. 1986.

Fang, H., Li, W. and Myneni, R. B.: The impact of potential land cover misclassification on MODIS leaf area index (LAI) estimation: A statistical perspective, **Remote Sens.**, 5, 810–829, doi:10.3390/rs5020810, 2013.

Farquhar, G. D., Caemmerer, S. Von and Berry, J. A.: A biogeochemical model of photosynthesis $CO_2$ assimilation in leaves of C3 species, **Plant**, 149, 78–90, 1980.

Favier, C., Chave, J., Fabing, A., Schwartz, D. and Dubois, M. A.: Modelling forest-savanna mosaic dynamics in man-influenced environments: Effects of fire, climate and soil heterogeneity, **Ecol. Modell.**, 171, 85–102, doi:10.1016/j.ecolmodel.2003.07.003, 2004.

Ferreira-Ribeiro, L. and Tabarelli, M.: A structural gradient in cerrado vegetation of Brazil: changes in woody plant density, species richness, life history and plant composition, **J. Trop. Ecol.**, 18(05), doi:10.1017/S026646740200250X, 2002.

Foley, J. A., Prentice, I. C., Ramankutty, N., Levis, S., Pollard, D., Sitch, S. and Haxeltine, A.: An integrated biosphere model of land surface processes, terrestrial carbon balance, and vegetation dynamics, **Global Biogeochem. Cycles**, 10, 603, doi:10.1029/96GB0 2692, 1996.

Friedl, M. A., Brodley, C. E. and Strahler, A. H.: Maximizing land cover classification accuracies produced by decision trees at continental to global scales, **IEEE Trans. Geosci. Remote Sens.**, 37, 969–977, doi:10.1109/36.752215, 1999.

Goll, D. S., Brovkin, V., Parida, B. R., Reick, C. H., Kattge, J., Reich, P. B., Van Bodegom, P. M. and Niinemets, Ü.: Nutrient limitation reduces land carbon uptake in simulations with a model of combined carbon, nitrogen and phosphorus cycling, **Biogeosciences**, 9(C), 3547–3569, doi:10.5194/bg-9-3547-2012, 2012.

Gonçalves, J. L. M.: **Cinética de transformação de fósforo lábil em não lábil em amostras de solos de Cerrado**, Tese (Mestrado em Solos e Nutrição de Plantas) - Viçosa -MG, Universidade Federal de Viçosa – UFV, 62p. 1988.

Gotsch, S. G., Geiger, E. L., Franco, A. C., Goldstein, G., Meinzer, F. C. and Hoffmann, W. A.: Allocation to leaf area and sapwood area affects water relations of co-occurring savanna and forest trees, **Oecologia**, 163(2), 291–301, doi:10.1007/s00442-009-1543-2, 2010.

Hansen, M. C. and Reed, B.: A comparison of the IGBP DISCover and University of Maryland 1km global land cover products, **Int. J. Remote Sens.**, 21, 1365–1373, doi:10.1080/014311600210218, 2000.

Hedley, M. J. and Stewart, J. W. B.: Method to measure microbial phosphate in soils, **Soil Biol. Biochem.**, 14, 377–385, doi:10.1016/0038-0717(82)90009-8, 1982.

Hirota, M., Nobre, C., Oyama, M. D. and Bustamante, M. M. C.: The climatic sensitivity of the forest, savanna and forest-savanna transition in tropical South America, **New Phytol.**, 187, 707–719, doi:10.1111/j.1469-8137.2010.03352.x, 2010.

Hoffmann, W. A., Adasme, R., Haridasan, M., De Carvalho, M. T., Geiger, E. L., Pereira, M. A. B., Gotsch, S. G. and Franco, A. C.: Tree topkill, not mortality, governs the dynamics of savanna-forest boundaries under frequent fire in central Brazil, **Ecology**, 90(5), 1326–1337, doi:10.1890/08-0741.1, 2009.

Hoffmann, W. A., Geiger, E. L., Gotsch, S. G., Rossatto, D. R., Silva, L. C. R., Lau, O. L., Haridasan, M. and Franco, A. C.: Ecological thresholds at the savanna-forest boundary: How

plant traits, resources and fire govern the distribution of tropical biomes, **Ecol. Lett.**, 15, 759–768, doi:10.1111/j.1461-0248.2012.01789.x, 2012.

Hoffmann, W. A., Da Silva, E. R., Machado, G. C., Bucci, S. J., Scholz, F. G., Goldstein, G. and Meinzer, F. C.: Seasonal leaf dynamics across a tree density gradient in a Brazilian savanna, **Oecologia**, 145, 307–316, doi:10.1007/s00442-005-0129-x, 2005.

House, J. I., Archer, S., Breshears, D. D. and Scholes, R. J.: Conundrums in mixed woody-herbaceous plant systems, **J. Biogeogr.**, 30, 1763–1777, doi:10.1046/j.1365-2699.2003.00873.x, 2003.

Jain, A. K., Kheshgi, H. S. and Wuebbles, D. J.: A globally aggregated reconstruction of cycles of carbon and its isotopes, Tellus, Ser. B Chem. **Phys. Meteorol.**, 48, 583–600, 1996.

Jain, A. K., Tao, Z., Yang, X. and Gillespie, C.: Estimates of global biomass burning emissions for reactive greenhouse gases (CO, NMHCs, and NOx) and $CO_2$, **J. Geophys. Res. Atmos.**, 111, doi:10.1029/2005JD006237, 2006.

Jain, A. K. and Yang, X.: Modeling the effects of two different land cover change data sets on the carbon stocks of plants and soils in concert with $CO_2$ and climate change, **Global Biogeochem. Cycles**, 19, n/a–n/a, doi:10.1029/2004GB002349, 2005.

Kattge, J., Knorr, W., Raddatz, T. and Wirth, C.: Quantifying photosynthetic capacity and its relationship to leaf nitrogen content for global-scale terrestrial biosphere models, **Glob. Chang. Biol.**, 15, 976–991, doi:10.1111/j.1365-2486.2008.01744.x, 2009.

Ker, J. C.: **Mineralogia, sorção e dessorção de fosfato, magnetização e elementos traços de Latossolos do Brasil**, Tese (Doutorado em Solos e Nutrição de Plantas) – Viçosa – MG, Universidade Federal de Viçosa – UFV, 181p. 1995.

Kucharik, C. J., Foley, J. A., Delire, C., Fisher, V. A., Coe, M. T., Lenters, J. D., Young-Molling, C., Ramankutty, N., Norman, J. M. and Gower, S. T.: Testing the performance of a Dynamic Global Ecosystem Model: Water balance, carbon balance, and vegetation structure, **Global Biogeochem. Cycles**, 14(3), 795–825, doi:10.1029/1999GB001138, 2000.

Lehmann, C. E. R., Archibald, S. A., Hoffmann, W. A. and Bond, W. J.: Deciphering the distribution of the savanna biome, **New Phytol.**, 191, 197–209, doi:10.1111/j.1469-8137.2011.03689.x, 2011.

Lloyd, J., Goulden, M. L., Ometto, J. P., Patiño, S., Fyllas, N. M. and C. A. Quesada: Ecophysiology of Forest and Savanna Vegetation, **Amaz. Glob. Chang.,** 451–462, doi:10.1029/2008GM000741, 2009.

Malavolta, E.: Nutrição mineral, In: **Fisiologia vegetal**, edited by M. G. Ferri, pp. 97–116, São Paulo, 1985.

Malhi, Y., Aragão, L. E. O. C., Metcalfe, D. B., Paiva, R., Quesada, C. A., Almeida, S., Anderson, L., Brando, P., Chambers, J. Q., da Costa, A. C. L., Hutyra, L. R., Oliveira, P., Patiño, S., Pyle, E. H., Robertson, A. L. and Teixeira, L. M.: Comprehensive assessment of carbon

productivity, allocation and storage in three Amazonian forests, **Glob. Chang. Biol.**, 15, 1255–1274, doi:10.1111/j.1365-2486.2008.01780.x, 2009.

Malhi, Y., Saatchi, S., Girardin, C. and Aragão, L. E. O. C.: The production, storage, and flow of carbon in Amazonian forests, **Geophys. Monogr. Ser.**, 186, 355–372, doi:10.1029/2008GM000779, 2009.

Malhi, Y., Wood, D., Baker, T. R., Wright, J., Phillips, O. L., Cochrane, T., Meir, P., Chave, J., Almeida, S., Arroyo, L., Higuchi, N., Killeen, T. J., Laurance, S. G., Laurance, W. F., Lewis, S. L., Monteagudo, A., Neill, D. a., Vargas, P. N., Pitman, N. C. a, Quesada, C. A., Salomão, R., Silva, J. N. M., Lezama, A. T., Terborgh, J., Martínez, R. V. and Vinceti, B.: The regional variation of aboveground live biomass in old-growth Amazonian forests, **Glob. Chang. Biol.**, 12, 1107–1138, doi:10.1111/j.1365-2486.2006.01120.x, 2006.

Marimon Junior, B. H. and Haridasan, M.: Comparação da vegetação arbórea e características edáficas de um cerradão e um cerrado sensu stricto em áreas adjacentes sobre solo distrófico no leste de Mato Grosso, Brasil, **Acta Bot. Brasilica**, 19(4), 913–926, doi:10.1590/S0102-33062005000400026, 2005.

McGrath, D. A., Smith, C. K., Gholz, H. L. and Oliveira, F. D. A.: Effects of land-use change on soil nutrient dynamics in Amazônia, **Ecosystems**, 4(May), 625–645, doi:10.1007/s10021-001-0033-0, 2001.

McWilliam, A.-L. C., Roberts, J. M., Cabral, O. M. R., Leitao, M. V. B. R., Costa, A. C. L. De, Maitelli, G. T. and Zamparoni, C. A. G. P.: Leaf Area Index and Above-Ground Biomass of terra firme Rain Forest and Adjacent Clearings in Amazonia, **Funct. Ecol.**, 7(3), 310 – 317, 1993.

Mendes, K. R., Marenco, R. A. and Magalhães, N. dos S.: Crescimento e eficiência fotossintética de uso do nitrogênio e fósforo em espécies florestais da Amazônia na fase juvenil, **Rev. Árvore**, 37(4), 707–716, doi:10.1590/S0100-67622013000400014, 2013.

Mercado, L. M., Lloyd, J., Dolman, A. J., Sitch, S. and Patiño, S.: Modelling basin-wide variations in Amazon forest productivity I. Model calibration, evaluation and upscaling functions for canopy photosynthesis, **Biogeosciences**, 6, 1247–1272, doi:10.5194/bgd-6-2965-2009, 2009.

Mercado, L. M., Patino, S., Domingues, T. F., Fyllas, N. M., Weedon, G. P., Sitch, S., Quesada, C. A., Phillips, O. L., Aragao, L. E. O. C., Malhi, Y., Dolman, A. J., Restrepo-Coupe, N., Saleska, S. R., Baker, T. R., Almeida, S., Higuchi, N. and Lloyd, J.: Variations in Amazon forest productivity correlated with foliar nutrients and modelled rates of photosynthetic carbon supply, **Philos. Trans. R. Soc. Lond. B. Biol. Sci.**, 366(1582), 3316–3329, doi:10.1098/rstb.2011.0045, 2011.

Miranda, A. C., Miranda, H. S., Lloyd, J., Grace, J., Francey, R. J., McIntyre, J. A., Meir, P., Riggan, P., Lockwood, R. and Brass, J.: Fluxes of carbon, water and energy over Brazilian cerrado: an analysis using eddy covariance and stable isotopes, **Plant, Cell Environ.**, 20, 315–328, 1997.

Miranda, I. S., Absy, M. L. and Rebêlo, G. H.: Community structure of woody plants of Roraima savannas, Brazil, **Plant Ecol.**, 164(1), 109–123, doi:10.1023/A:102129 8328048, 2003.

Moreira, J. F.: **Cinética de transformação de P-lábil em não-lábil no solo avaliada por análise química e crescimento de mudas de eucalipto**, Tese (Mestrado em Solos e Nutrição de Plantas) – Viçosa – MG, Universidade Federal de Viçosa – UFV, 52 p. 1988.

Muniz, A. S.: **Disponibilidade de fósforo avaliada por extratores químicos e pelo crescimento de soja (Glycine max (L.) Merrill) em amostras de solo com diferentes valores do fator capacidade**, Tese (Mestrado em Solos e Nutrição de Plantas) – Viçosa – MG, Universidade Federal de Viçosa – UFV, 79 p. 1983.

Murphy, B. P. and Bowman, D. M. J. S.: What controls the distribution of tropical forest and savanna?, **Ecol. Lett.,** 15, 748–758, doi:10.1111/j.1461-0248.2012.01771.x, 2012.

Neves, J. C. L.: **Produção e partição de biomassa, aspectos nutricionais e hídricos em plantios clonais de eucalipto na região litorânea do Espírito Santo**, Tese (Doutorado em Produção Vegetal) – Campos dos Goytacazes – RJ, Universidade Estadual do Norte Fluminense – UENF, 191 p. 2000.

New, M., Hulme, M. and Jones, P.: Representing Twentieth-Century Space – Time Climate Variability. Part I : Development of a 1961 – 90 Mean Monthly Terrestrial Climatology, **J. Clim**., 12, 829–856, doi:10.1175/1520-0442(1999)012<0829:RTCSTC> 2.0.CO;2, 1999.

Nogueira, E. M., Yanai, A. M., Fonseca, F. O. and Fearnside, P. M.: Carbon stock loss from deforestation through 2013 in Brazilian Amazonia., **Glob. Chang. Biol.**, doi:10.1111/gcb.12798, 2014.

Novelino, J. O.: **Disponibilidade de fósforo e sua cinética em solos sob cerrado fertilizados com fósforo, avaliada por diferentes métodos de extração**, Tese (Doutorado em Solos e Nutrição de Plantas) ) – Viçosa – MG, Universidade Federal de Viçosa – UFV, 70p. 1999.

Oleson, K. W., Dai, Y., Bonan, G. B., Bosilovich, M., Dickinson, R. E., Dirmeyer, P., Dirmeyer, P., Hoffman, F., Houser, P., Levis, S., Niu, G.-Y., Thornton, P., Vertenstein, M., Yang, Z.-L. and Zeng, X.: Technical Description of the Community Land Model (CLM), **NCAR Tech. Note**, NCAR/TN-46, 186, 2004.

Oyama, M. D. and Nobre, C. A.: A new climate-vegetation equilibrium state for Tropical South America, **Geophys. Res. Lett.**, 30(23), 10–13, doi:10.1029/2003GL018600, 2003.

Paoli, G. D., Curran, L. M. and Slik, J. W. F.: Soil nutrients affect spatial patterns of aboveground biomass and emergent tree density in southwestern Borneo, **Oecologia**, 155, 287–299, doi:10.1007/s00442-007-0906-9, 2008.

Parton, W. J., Scurlock, J. M. O., Ojima, D. S., Gilmanov, T. G., Scholes, R. J., Schimel, D. S., Kirchner, T., Menaut, J.-C., Seastedt, T., Garcia Moya, E., Kamnalrut, A. and Kinyamario, J. I.: Observations and modeling of biomass and soil organic matter dynamics for the grassland biome worldwide, **Global Biogeochem. Cycles**, 7, 785, doi:10.1029/93GB02042, 1993.

Paula, J. R.: **Avaliação da disponibilidade de fósforo por extratores orgânicos em latossolos de Minas Gerais**, Tese (Mestrado em Solos e Nutrição de Plantas) ) – Viçosa – MG, Universidade Federal de Viçosa – UFV, 58 p. 1993.

Phillips, O. L., Baker, T. R., Arroyo, L., Higuchi, N., Killeen, T. J., Laurance, W. F., Lewis, S. L., Lloyd, J., Malhi, Y., Monteagudo, A., Neill, D. A., Vargas, P. N., Silva, J. N. M., Terborgh, J., Martínez, R. V., Alexiades, M., Almeida, S., Brown, S., Chave, J., Comiskey, J. A., Czimczik, C. I., Di Fiore, A., Erwin, T., Kuebler, C., Laurance, S. G., Nascimento, H. E. M., Olivier, J., Palacios, W., Patiño, S., Pitman, N. C. A., Quesada, C. A., Saldias, M., Lezama, A. T. and Vinceti, B.: Pattern and process in Amazon tree turnover, 1976-2001., **Philos. Trans. R. Soc. Lond. B. Biol. Sci.**, 359(1443), 381–407, doi:10.1098/rstb.2003.1438, 2004.

Poggiani, F.: Ciclagem de nutrientes e manutenção da produtividade da floresta plantada, In: Fundação Centro Tecnológico de Minas Gerais. **Gaseificação de madeira e carvão vegetal**, pp. 25–33, Belo Horizonte. 1981.

Quesada, C. A., Lloyd, J., Anderson, L. O., Fyllas, N. M., Schwarz, M. and Czimczik, C. I.: Soils of Amazonia with particular reference to the RAINFOR sites, **Biogeosciences**, 8, 1415–1440, doi:10.5194/bg-8-1415-2011, 2011.

Quesada, C. A., Lloyd, J., Schwarz, M., Baker, T. R., Phillips, O. L., Patiño, S., Czimczik, C., Hodnett, M. G., Herrera, R., Arneth, A., Lloyd, G., Malhi, Y., Dezzeo, N., Luizão, F. J., Santos, A. J. B., Schmerler, J., Arroyo, L., Silveira, M., Priante Filho, N., Jimenez, E. M., Paiva, R., Vieira, I., Neill, D. A., Silva, N., Peñuela, M. C., Monteagudo, A., Vásquez, R., Prieto, A., Rudas, A., Almeida, S., Higuchi, N., Lezama, A. T., López-González, G., Peacock, J., Fyllas, N. M., Alvarez Dávila, E., Erwin, T., di Fiore, A., Chao, K. J., Honorio, E., Killeen, T., Peña Cruz, A., Pitman, N., Núñez Vargas, P., Salomão, R., Terborgh, J. and Ramírez, H.: Regional and large-scale patterns in Amazon forest structure and function are mediated by variations in soil physical and chemical properties, **Biogeosciences Discuss**., 6, 3993–4057, doi:10.5194/bgd-6-3993-2009, 2009.

Quesada, C. A., Lloyd, J., Schwarz, M., Patiño, S., Baker, T. R., Czimczik, C., Fyllas, N. M., Martinelli, L., Nardoto, G. B., Schmerler, J., Santos, a. J. B., Hodnett, M. G., Herrera, R., Luizão, F. J., Arneth, A., Lloyd, G., Dezzeo, N., Hilke, I., Kuhlmann, I., Raessler, M., Brand, W. A., Geilmann, H., Filho, J. O. M., Carvalho, F. P., Filho, R. N. A., Chaves, J. E., Cruz, O. F., Pimentel, T. P. and Paiva, R.: Variations in chemical and physical properties of Amazon forest soils in relation to their genesis, **Biogeosciences**, 7, 1515–1541, doi:10.5194/bg-7-1515-2010, 2010.

Ramankutty, N. and Foley, J. A.: Estimating historical changes in global land cover: Croplands from 1700 to 1992, **Global Biogeochem. Cycles**, 13, 997–1027, doi:10.1029/1999GB900046, 1999.

Ratnam, J., Bond, W. J., Fensham, R. J., Hoffmann, W. A., Archibald, S., Lehmann, C. E. R., Anderson, M. T., Higgins, S. I. and Sankaran, M.: When is a "forest" a savanna, and why does it matter?, **Glob. Ecol. Biogeogr.**, 20(5), 653–660, doi:10.1111/j.1466-8238.2010.00634.x, 2011.

Reich, P. B., Walters, M. B., Kloeppel, B. D. and Ellsworth, D. S.: Different photosynthesis-nitrogen relations in deciduous hardwood and evergreen coniferous tree species, **Oecologia**, 104, 24–30, doi:10.1007/BF00365558, 1995.

Ribeiro, J. F. and Walter, B. M. T.: As Principais Fitofisionomias do bioma Cerrado, in **Cerrado: ecologia e flora**, pp. 153–212., 2008.

Salazar, L. F., Nobre, C. A. and Oyama, M. D.: Climate change consequences on the biome distribution in tropical South America, **Geophys. Res. Lett.**, 34(April), 2–7, doi:10.1029/2007GL029695, 2007.

Sankaran, M., Ratnam, J. and Hanan, N. P.: Tree-grass coexistence in savannas revisited – Insights from an examination of assumptions and mechanisms invoked in existing models, **Ecol. Lett.**, 7, 480–490, doi:10.1111/j.1461-0248.2004.00596.x, 2004.

Dos Santos, F. C., Neves, J. C. L., Novais, R. F., Alvarez, V.H. and Sediyama, C. S.: Modelagem da recomendação de corretivos e fertilizantes para a cultura da soja, **Rev. Bras. Cienc. do Solo**, 32(1), 1661–1674, doi:10.1590/S0100-06832008000400031, 2008.

Scepan, J.: Thematic validation of high-resolution global land-cover data sets, **Photogramm. Eng. Remote Sensing**, 65, 1051–1060, 1999.

Sharkey, T. D.: Photosynthesis in intact leaves of C3 plants: Physics, physiology and rate limitations, **Bot. Rev.**, 51, 53–105, doi:10.1007/BF02861058, 1985.

Shukla, J., Nobre, C. and Sellers, P.: Amazon deforestation and climate change, **Science**, 247, 1322–1325, doi:10.1126/science.247.4948.1322, 1990.

Silver, W. L., Scatena, F. N., Johnson, A. H., Siccama, T. G. and Sanchez, M. J.: Nutrient availability in a montane wet tropical forest: Spatial patterns and methodological considerations, **Plant Soil**, 164, 129–145, doi:10.1007/BF00010118, 1994.

Silvério, D. V, Brando, P. M., Balch, J. K., Putz, F. E., Nepstad, D. C., Oliveira-Santos, C. and Bustamante, M. M. C.: Testing the Amazon savannization hypothesis: fire effects on invasion of a neotropical forest by native cerrado and exotic pasture grasses, **Philos. Trans. R. Soc. Lond. B. Biol. Sci.**, 368, 20120427, doi:10.1098/rstb.2012.0427, 2013.

Sitch, S., Smith, B., Prentice, I. C., Arneth, A., Bondeau, A., Cramer, W., Kaplan, J. O., Levis, S., Lucht, W., Sykes, M. T., Thonicke, K. and Venevsky, S.: Evaluation of ecosystem dynamics, plant geography and terrestrial carbon cycling in the LPJ dynamic global vegetation model, **Glob. Chang. Biol.**, 9, 161–185, doi:10.1046/j.1365-2486.2003.00569.x, 2003.

Smith, B., Prentice, I. C. and Sykes, M. T.: Representation of vegetation dynamics in the modelling of terrestrial ecosystems: Comparing two contrasting approaches within European climate space, **Glob. Ecol. Biogeogr.**, 10, 621–637, doi:10.1046/j.1466-822X.2001.00256.x, 2001.

Switzer, G. L. and Nelson, L. E.: Maintenance of productivity under short rotations, In: **International Symposium on Forest Fertilization**, pp. 365–389, Paris., 1973.

Thompson, S. L. and Pollard, D.: A global climate model (GENESIS) with a land-surface transfer scheme (LSX). Part I: present climate simulation, **J. Clim.**, 8, 732–761, doi:10.1175/1520-0442(1995)008<0732:AGCMWA>2.0.CO;2, 1995.

Torello-Raventos, M., Feldpausch, T., Veenendaal, E., Schrodt, F., Saiz, G., Domingues, T., Djagbletey, G., Ford, A., Kemp, J., Marimon, B., Hur Marimon Junior, B., Lenza, E., Ratter, J., Maracahipes, L., Sasaki, D., Sonké, B., Zapfack, L., Taedoumg, H., Villarroel, D., Schwarz, M.,

Quesada, C., Yoko Ishida, F., Nardoto, G., Affum-Baffoe, K., Arroyo, L., Bowman, D., Compaore, H., Davies, K., Diallo, A., Fyllas, N., Gilpin, M., Hien, F., Johnson, M., Killeen, T., Metcalfe, D., Miranda, H., Steininger, M., Thomson, J., Sykora, K., Mougin, E., Hiernaux, P., Bird, M., Grace, J., Lewis, S., Phillips, O. and Lloyd, J.: On the delineation of tropical vegetation types with an emphasis on forest/savanna transitions, **Plant Ecol. Divers.**, 6, 101–137, doi:10.1080/17550874.2012.76281, 2013.

Uehara, G. and Gillman, G.: The Mineralogy, Chemistry, and Physics of Tropical Soils with Variable Charge Clays, **Soil Sci.**, 139(4), 380, doi:10.1097/00010694-198504000-00019, 1985.

Verberne, E. L. J., Hassink, J., De Willigen, P., Groot, J. J. R. and Van Veen, J. A.: Modelling organic matter dynamics in different soils, **Netherlands J. Agric. Sci.**, 38, 221–238, 1990.

Walker, A. P., Beckerman, A. P., Gu, L., Kattge, J., Cernusak, L. A., Domingues, T. F., Scales, J. C., Wohlfahrt, G., Wullschleger, S. D. and Woodward, F. I.: The relationship of leaf photosynthetic traits - Vcmax and Jmax - to leaf nitrogen, leaf phosphorus, and specific leaf area: a meta-analysis and modeling study, **Ecol. Evol.**, 4(16), 3218–3235, doi:10.1002/ece3.1173, 2014.

Wang, Y. P., Law, R. M. and Pak, B.: A global model of carbon, nitrogen and phosphorus cycles for the terrestrial biosphere, **Biogeosciences**, 7, 2261–2282, doi:10.5194/bg-7-2261-2010, 2010.

Waring, R. H. and Schlesinger, W. H.: Hydrology of Forest Ecosystems, In: **Forest Ecosystems: Concepts and Management**, pp. 94–120., 1985.

Whittaker, R. H.: **Communities and ecosystems**, 2ª.edition by Macmillan, New York, USA, 1975.

Woodward, F. I., Smith, T. M. and Emanuel, W. R.: A global land primary productivity and phytogeography model, **Global Biogeochem. Cycles**, 9, 471–490, doi:10.1029/95G B02432, 1995.

Wright, S. J.: Tropical forests in a changing environment, **Trends Ecol. Evol.**, 20(10), 553–560, doi:10.1016/j.tree.2005.07.009, 2005.

Yang, X. and Post, W. M.: Phosphorus transformations as a function of pedogenesis: A synthesis of soil phosphorus data using Hedley fractionation method, **Biogeosciences**, 8, 2907–2916, doi:10.5194/bg-8-2907-2011, 2011.

Yang, X., Post, W. M., Thornton, P. E. and Jain, A.: The distribution of soil phosphorus for global biogeochemical modeling, **Biogeosciences**, 10, 2525–2537, doi:10.5194/bg-10-2525-2013, 2013.

Yang, X., Thornton, P. E., Ricciuto, D. M. and Post, W. M.: The role of phosphorus dynamics in tropical forests - A modeling study using CLM-CNP, **Biogeosciences**, 11, 1667–1681, doi:10.5194/bg-11-1667-2014, 2014.

## 5. APPENDIX A

**Table A1.** Phosphorus samples in $P_{resin}$ and clay fraction to different plots in the Brazilian Amazon from the database Quesada et al. (2010).

| **Plot** | **Location** | | **$P_{Resin}$** | **$P_{total}$** | **Clay** |
|---|---|---|---|---|---|
| ID | Latitude | Longitude | mg $kg^{-1}$ | mg $kg^{-1}$ | % |
| 'RIO-12' | 8.5 | -61.5 | 3.42 | 178.96 | 9.50 |
| 'ELD-12' | 6.5 | -61.5 | 5.34 | 173.59 | 20.13 |
| 'SCR-01' | 1.5 | -67.5 | 2.36 | 65.85 | 6.88 |
| 'TIP-05' | -0.5 | -76.5 | 9.01 | 437.32 | 37.30 |
| 'JRI-01' | -0.5 | -52.5 | 1.30 | 189.13 | 80.73 |
| 'JAS-02' | -1.5 | -77.5 | 8.79 | 423.65 | 29.13 |
| 'CAX-01' | -1.5 | -51.5 | 5.17 | 115.18 | 41.77 |
| 'MBO-01' | -1.5 | -48.5 | 3.14 | 101.38 | 11.49 |
| 'BNT-04' | -2.5 | -60.5 | 4.82 | 68.67 | 57.68 |
| 'TAP-04' | -2.5 | -54.5 | 4.50 | 192.34 | 89.25 |
| 'ALP-12' | -3.5 | -73.5 | 7.37 | 86.62 | 13.96 |
| 'SUC-02' | -3.5 | -72.5 | 4.06 | 349.81 | 37.21 |
| 'AGP-01' | -3.5 | -70.5 | 2.99 | 303.28 | 42.61 |
| 'ZAR-03' | -3.5 | -69.5 | 4.81 | 177.19 | 31.11 |
| 'TAP-123' | -3.5 | -54.5 | 1.65 | 78.89 | 66.10 |
| 'ZAR-04' | -4.5 | -69.5 | 7.48 | 54.15 | 18.26 |
| 'JUR-01' | -8.5 | -72.5 | 10.55 | 331.93 | 36.62 |
| 'RST-01' | -9.5 | -72.5 | 8.29 | 240.19 | 25.40 |
| 'ALF-01' | -9.5 | -55.5 | 3.51 | 118.14 | 11.43 |
| 'DOI-01' | -10.5 | -68.5 | 7.18 | 203.19 | 19.09 |
| 'SIN-01' | -11.5 | -55.5 | 2.58 | 61.25 | 9.80 |
| 'TAM-01' | -12.5 | -69.5 | 5.85 | 343.51 | 37.75 |
| 'CUZ-03' | -12.5 | -68.5 | 11.45 | | 42.46 |
| 'CRP-01' | -14.5 | -61.5 | 21.82 | | 18.05 |
| 'HCC-21' | -14.5 | -60.5 | 7.34 | 289.76 | 25.60 |

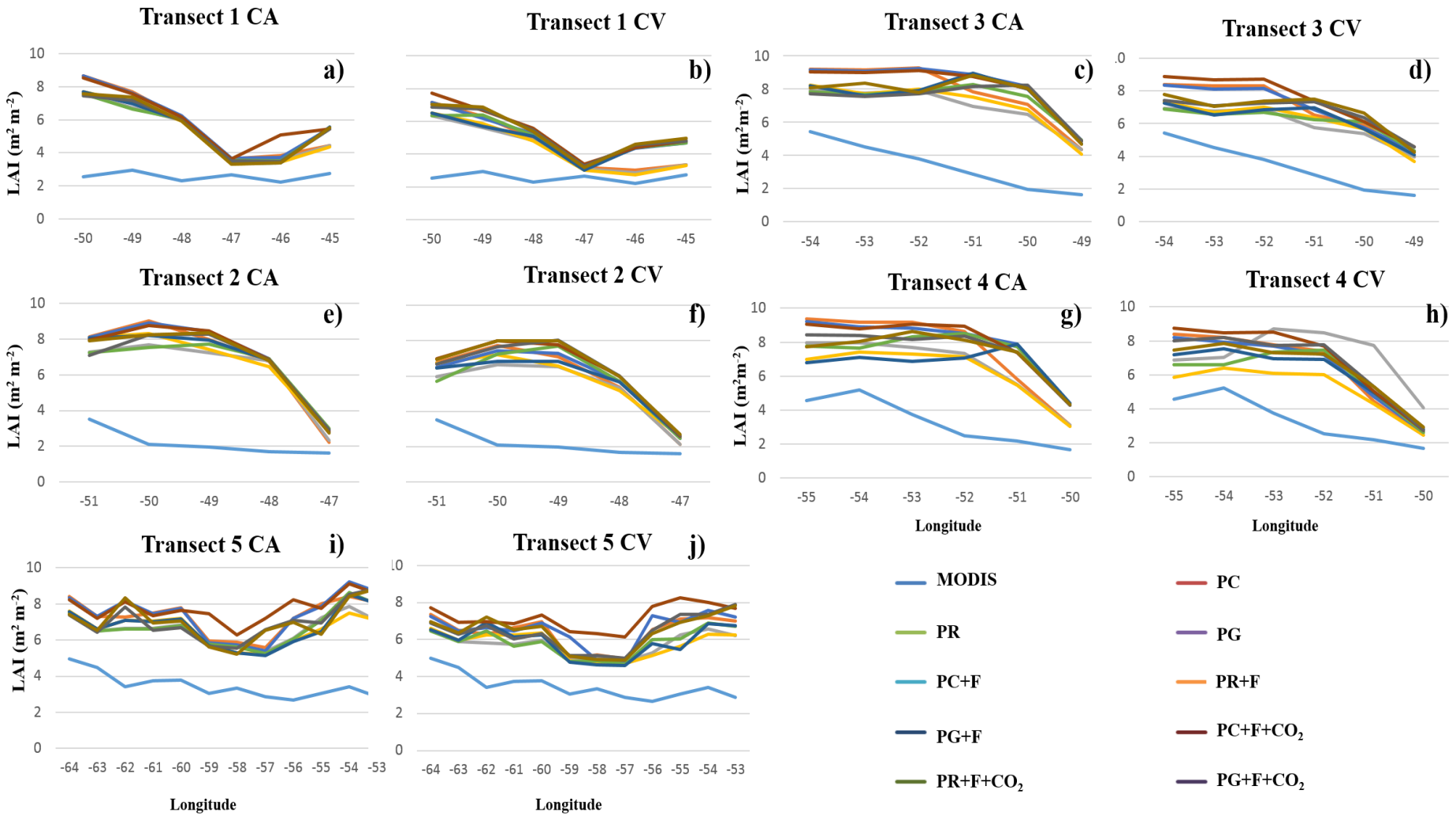


**Figure A1.** LAI observed and simulated for the five transects in the Amazon-Cerrado transition.

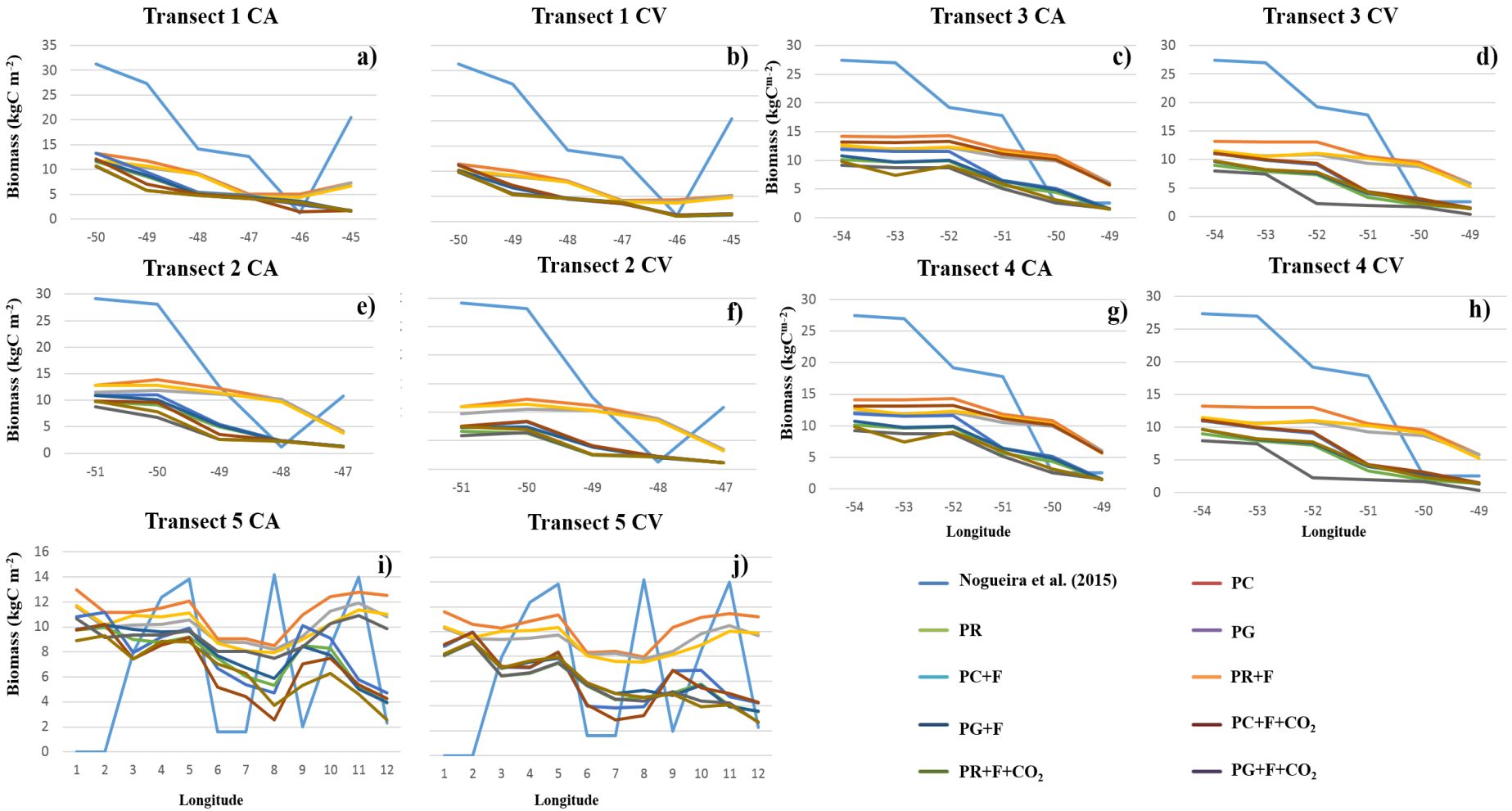


**Figure A2.** Biomass observed and simulated for the five transects in the Amazon-Cerrado transition.